

**Characterization of a Pseudomonad 2-Nitrobenzoate Nitroreductase and its
Catabolic Pathway Associated 2-Hydroxylaminobenzoate Mutase and a
Chemoreceptor Involved in 2-Nitrobenzoate Chemotaxis†**

HIROAKI IWAKI,¹ TAKAMICHI MURAKI,^{1,2} SHUN ISHIHARA,¹ YOSHIE
HASEGAWA,^{1*} KATHRYN N. RANKIN,² TRAIAN SULEA,² JASON BOYD,² and
PETER C.K. LAU^{2**}

*Department of Biotechnology, Faculty of Engineering and High Technology Research
Center, Kansai University, Suita, Osaka 564-8680, Japan,¹ and Biotechnology
Research Institute, National Research Council Canada, Montreal, Quebec H4P 2R2,
Canada²*

*Corresponding authors. Mailing address for Yoshie Hasegawa: Department of
Biotechnology, Faculty of Engineering and High Technology Research Center,
Kansai University, Suita, Osaka 564-8680, Japan. Phone: 81(6) 6368-0909. Fax:
81(6) 6388-8609. E-mail: yoshie@ipcku.kansai-u.ac.jp.

**Mailing address for Peter C.K. Lau: National Research Council Canada,
Biotechnology Research Institute, 6100 Royalmount Ave, Montreal, Quebec, H4P
2R2, Canada. Phone: Tel: (514) 496-6325. Fax: (514) 496-6265. E-mail:
peter.lau@cnrc-nrc.gc.ca.

†This publication is issued as NRCC number XXXXX.

Running title: 2-NITROBENZOATE METABOLISM AND CHEMOTAXIS

1 *Pseudomonas fluorescens* strain KU-7 is a prototype microorganism that
2 metabolizes 2-nitrobenzoate (2-NBA) via the formation of 3-hydroxyanthranilate
3 (3-HAA), a known antioxidant and reductant. The initial two steps leading to the
4 sequential formation of 2-hydroxyaminobenzoic acid (2-HABA) and 3-HAA are
5 catalyzed by a NADPH-dependent 2-nitrobenzoate nitroreductase (NbaA) and
6 2-hydroxylaminobenzoate mutase (NbaB), respectively. The 216-amino acid
7 protein NbaA is 78% identical to a plasmid-encoded hypothetical conserved
8 protein of *Polaromonas* strain JS666; structurally it belongs to the homodimeric
9 NADH:FMN oxidoreductase-like fold family. Structural modeling of complexes
10 with the flavin, coenzyme and substrate suggested specific residues contributing
11 to the NbaA catalytic activity, assuming a ping-pong reaction mechanism.
12 Mutational analysis supports the roles of Asn40, Asp76 and Glu113 predicted to
13 form the binding site for a divalent metal ion implicated in FMN binding, and a
14 role in NADPH binding for the 10-residue insertion in the β 5- α 2 loop. The
15 181-amino acid sequence of NbaB is 35% identical to the
16 4-hydroxylaminobenzoate lyases (PnbBs) of various 4-nitrobenzoate assimilating
17 bacteria, e.g., *P. putida* strain TW3. Co-expression of *nbaB* with *nbaA* in
18 *Escherichia coli* produced a small amount of 3-HAA from 2-NBA, supporting the
19 functionality of the *nbaB* gene. We also showed by gene knockout and chemotaxis
20 assay that *nbaY*, a chemoreceptor NahY homolog located downstream of the *nbaA*
21 gene, is responsible for strain KU-7 to be attracted toward 2-NBA. NbaY is the
22 first identified chemoreceptor in nitroaromatic metabolism, and this study
23 completes the gene elucidation of 2-NBA metabolism that is localized within a
24 24-kb chromosomal locus of strain KU-7.

1 **Nitroreduction, catalyzed by the NAD(P)H-dependent nitroreductases, is the**
2 **quintessential first step in the catabolism of a variety of structurally diverse**
3 **nitroaromatic compounds.** The commonly known oxygen-insensitive and type I
4 nitroreductases are flavoproteins that mediate the sequential transfer of two electrons
5 from NAD(P)H to the nitro group to produce nitroso and hydroxylamine derivatives
6 (9). From the hydroxylamine intermediate, ammonium ions are subsequently removed
7 through two possible routes: a lyase-mediated reaction with the direct elimination of
8 ammonia to produce the corresponding catechol (e.g. degradation of 4-nitrobenzoate,
9 4-nitrotoluene, and 3-nitrophenol); and a mutase-mediated Bamberger-type
10 rearrangement to produce 2-aminophenols or benzoates resulting in a much later
11 release of ammonia (e.g., metabolism of nitrobenzene, 3-nitrophenol,
12 4-chloronitrobenzene, 4-nitrotoluene, and 2,4,6-trinitrotoluene). For recent reviews
13 see Esteve-Nunez et al (20) and Nishino and Spain (51).

14 The metabolism of 2-nitrobenzoate (2-NBA) by *Pseudomonas fluorescens* strain
15 KU-7 afforded the first example in a prokaryotic organism for the formation of
16 3-hydroxyanthranilate (3-HAA), a metabolite that is otherwise well known in the
17 kynurenine pathway of tryptophan metabolism, and the biosynthesis of nicotinic acid
18 in yeast and mammalian systems (27, 49, 53). This organism is unable to grow on
19 3-nitrobenzoate or nitrophenols as sole carbon or nitrogen source (27). Recently,
20 Colabroy and Begley (15) identified a new tryptophan catabolic pathway in
21 *Burkholderia cepacia* J2315 that includes the formation of 3-HAA. Crude extracts of
22 strain KU-7 cells converted 2-NBA to 3-HAA with oxidation of 2 mol of NADPH. In
23 this pathway, 2-NBA is first reduced to 2-hydroxyaminobenzoic acid (2-HABA) by an
24 uncharacterized NADPH-dependent reductase, followed by a mutase-catalyzed
25 conversion of 2-HABA to 3-HAA via a Bamberger-type rearrangement (27).
26 Previously, we have described the genetic locus, consisting of *nbaEXHJIGFCDR*, that

1 is responsible for the conversion of 3-HAA to Krebs cycle intermediate in strain KU-7
2 (49). A highlight of this pathway is establishment of the novel identity of *nbaC*
3 encoding 3-hydroxyanthranilate 3,4-dioxygenase, and *nbaD* encoding
4 2-amino-3-carboxymuconate 6-semialdehyde decarboxylase, that catalyze respectively,
5 the ring-opening of 3-HAA to form 2-amino-3-carboxymuconate-6-semialdehyde and
6 a decarboxylation step to form 2-aminomuconate-6-semialdehyde (49). The latter
7 compound is a convergent metabolite in the metabolism of nitrobenzene,
8 2-aminophenol, 3-HAA and 4-amino-3-hydroxybenzoic acid (49, 52).

9 To complete the full gene complement for 2-NBA metabolism in strain KU-7, we
10 describe here the gene localization and characterization by nucleotide sequencing and
11 functional analysis of initial genes *nbaA* and *nbaB* encoding 2-NBA nitroreductase
12 and 2-HABA mutase, respectively. In particular, a homology model of NbaA was built
13 to probe the structure-function relationship of this protein. Additionally, we
14 determined the chemotactic property of a methyl-accepting chemotaxis transducer-like
15 open-reading frame (*nbaY*) that is located downstream of *nbaA*. This study has also
16 led to the discovery of a related gene locus in the *Polaromonas* sp. JS666 genome
17 (Joint Genome Institute [JGI] database), an organism known to degrade
18 *cis*-dichloroethene. The possible mobility of the *nba* gene locus is discussed.

19 (A portion of this work was presented at the American Society for Microbiology 9th
20 International Conference on *Pseudomonas*, Quebec City, Canada, 6 to 10 September,
21 2003).

22

23

MATERIALS AND METHODS

24 **Chemicals.** 2-HABA were synthesized chemically as described by Bauer and
25 Rosenthal (5). All other chemicals were of the highest purity commercially available.

26 **Bacterial strains, culture conditions, and plasmids.** The bacterial strains and

1 plasmids used in this study are listed in Table 1. The culture conditions for the
2 *Pseudomonas* and *E. coli* strains, their growth media except for MS-S medium (MY
3 medium without the yeast extract and 2-NBA but replaced with 0.3% succinate) and
4 antibiotic selection, are as previously described (27, 49).

5 **DNA manipulations, sequencing and analysis.** Chromosomal and plasmid DNA
6 isolation used the methods of Wilson, and Birnboim and Doly, respectively, as
7 referenced in Muraki et al (49). Purification of DNA fragment, labelling with
8 digoxigenin (DIG)-11-dUTP using the DIG DNA Labeling Kit, and visualization with
9 a DIG Luminescent Detection kit (Roche Diagnostics K.K., Tokyo) were as previously
10 described (27, 49). Southern blotting used a positively charged nylon membrane
11 (Hybond-N+; Amersham Biosciences Corp., Piscataway, NJ) and other DNA
12 manipulations such as DNA ligation are as described in Sambrook et al. (61).
13 Restriction endonucleases and T4 DNA ligase were from New England Biolabs
14 (Beverly, Mass). Automated and BigDye terminator nucleotide sequencing were used
15 as before (49). DNA and protein sequence analyses were carried out using the
16 GENETYX-Mac software (Software Development Co., Ltd., Tokyo) as well as the
17 BLAST programs at the National Center for Biotechnology Information (NCBI) server.
18 (2).

19 **Transposon mutagenesis and screening for 2-NBA-negative mutant strains.**
20 Transposon mutagenesis was carried out in order to gain access to the 2-NBA
21 catabolic pathway gene locus by the generation of mutant derivatives of strain KU-7
22 that are unable to grow on 2-NBA as a sole carbon source. As previously described
23 (49), pKN31 was used as a delivery vehicle for transposon Tn5-31/Tp and *E. coli* strain
24 S17-1 as a donor in conjugation with the wildtype KU-7 for the construction of strains
25 KUM-4 etc (Table 1). Kanamycin (Km, 50 µg/ml) was used as a selective marker for
26 the transposon. Transconjugants of strain KU-7 were identified following incubation at

1 30°C for 2 days. Mutants that were not able to grow on 2-NBA were identified by
2 replica plating on MS medium containing 0.2% 2-NBA (12 mM) and Km as previously
3 described (49).

4 Amplification of Tn5-3/Tp flanking fragments by inverse PCR (IPCR) was
5 performed using the method of Huang et al. (30). Total DNA prepared from Tn5-3/Tp
6 mutant of strain KU-7 was digested with *Bam*HI to cut the middle of the Tn5-3/Tp
7 and the *Bam*HI recognition sequence flanking the transposon insertion site. Following
8 phenol:chloroform extraction and ethanol precipitation, the digested DNA was
9 self-ligated in a final volume of 1 ml at a concentration of 0.3-0.5 µg in the presence
10 of 3 U T4 DNA ligase (New England Biolabs) overnight at 16°C. The ligation mixture
11 was extracted with phenol:chloroform, precipitated with ethanol, and resuspended in
12 sterile distilled H₂O to a concentration of 20 ng µl⁻¹. To amplify the flanking
13 sequences of Tn5-3/Tp insertion, a set of two parallel IPCR reactions using the
14 ligation mixture as template were performed using primers BL and IR1, and BR and
15 IR1. The BL and BR primers (5'-GGGGACCTTGCACAGATAGC and 5'-
16 CATTCTGTAGCGGATGGAGATC, respectively) are sequences on both sides of the
17 unique *Bam*HI site of the transposon; IR1 primer
18 (5'-GAGCAGAAGTTATCATGAACG) is based on the terminal inverted repeats (IR)
19 of Tn5-3/Tp. IPCR was performed in a volume of 25 µl with 25 ng DNA of ligation
20 mixture, 7.5 pmol of each primer, 200 µM of each dNTP, 2.5 µl of GeneAmp High
21 Fidelity 10X PCR buffer with MgCl₂, and 0.25 µl of GeneAmp High Fidelity enzyme
22 mix (Applied Biosystems). For amplification, a 2 min initial denaturation step at 94°C
23 was followed by 30 thermal cycles of denaturation at 94°C for 15s, annealing at 50°C
24 for 1 min and extension at 68°C for 8 min. The PCR product was purified from a 1.0%
25 agarose gel and sequence reaction was performed with IR1 primer.

1 **Construction of *nbaY* deletion mutant.** A crossover PCR deletion product of *nbaY*
2 was constructed as follows, based on the same strategy as PCR overlap extension
3 mutagenesis according to Link et al (47). Supplemental Fig. S1 depicts the strategy. At
4 first, two different asymmetric PCRs were used to generate fragments to the left and
5 right of *nbaY* with the following pairs of PCR primers: *nbaY*-Co,
6 5'-CGGAATTCGC^GAACTGCTGGACGTGCCT-3' and *nbaY*-Ci,
7 5'-TGTTTAAGTTTAGTGGATGGGGACCTGAGTCAGCTGTTAGG-3', and
8 *nbaY*-Ni, 5'-CCCATCCACTAAACTTAAACAATTACGTAAACTAGTCACCG-3',
9 and *nbaY*-No, 5'-CGGAATTCTATCTCAGAAGCCGAAGCCG-3', respectively. The
10 left and right fragments were then annealed at their overlapping region (double
11 underlined complementary sequences) and amplified by PCR as a single fragment,
12 using the primers *nbaY*-Co and *nbaY*-No. The crossover PCR deletion product was
13 subcloned into the *EcoRI* site of pK18*mobsacB*, generating pNbaΔ*Y*. To facilitate this
14 cloning, *EcoRI* recognition sites were introduced in the primer design of *nbaY*-Co and
15 *nbaY*-No as underlined above.

16 Plasmid pNbaΔ*Y* was transferred into strain KU-7 by conjugation with *E. coli*
17 S17-1 as described earlier. Transconjugants were first selected on MS-S agar
18 containing Km. These transconjugants were not able to grow on MS-S agar containing
19 10% sucrose since the levansucrase-encoding gene (*sacB*) on the pK18*mobsacB* vector
20 when expressed would provide a lethal phenotype to the cells growing on sucrose (18,
21 23). To select for a double cross-over event, a single colony was grown for 18 hrs in a
22 non-selective MS-S medium at 30°C. The cells were plated onto MS-S agar containing
23 10% sucrose and incubated for 24 hrs at 30°C. The resulting colonies were sensitive to
24 Km, indicating the excision of the plasmid by a second cross-over event. This second
25 cross-over either restores the wild type situation or leads to a mutant with the desired
26 deletion. The deletion mutants were analyzed by PCR and designated strain KU-Δ*Y*.

1 **Subcloning of *nbaA* and *nbaB* and expression in *E. coli*.** The DNA fragment
 2 carrying *nbaA* and *nbaB* were amplified from KU-7 genomic DNA by using
 3 KOD-Plus-DNA polymerase (Toyobo) with the following pairs of PCR primers, and
 4 the desired restriction sites (*EcoRI* and *PstI* [underlined sequences]) to facilitate
 5 subsequent cloning: *nbaA*, 5'-CGGAATTCATGACGCACATTGCAATGTCA and
 6 5'-AAAACTGCAGTCAGGGAGTAATCGGAAAGA. *nbaB*,
 7 5'-CGGAATTCATGTCCAATGCCCCGAATGCA and
 8 5'-AAAACTGCAGTGAGTATTGTCAGGAAGT.

9 In each case, the amplified DNA fragment was purified from an agarose gel,
 10 digested with the appropriate restriction enzymes, and cloned in the linearized pSD80
 11 *tac*-inducible expression vector (66). The resultant recombinant plasmids were
 12 designated pSD*nbaA* and pSD*nbaB* (Table 1). DNA sequencing was performed to
 13 exclude the possibility of mutations of the amplified genes. The plasmid carrying *E.*
 14 *coli* BL21 cells were cultivated in 100 ml of LB medium containing 100 µg of Ap/ml
 15 at 30°C. When the culture reached an A_{600} of 0.3 to 0.4,
 16 isopropyl-β-thio-D-galactoside (IPTG) was added to a final concentration of 1 mM in
 17 the medium. The cells were further cultured for 3 h, harvested by centrifugation,
 18 washed twice with 50 mM potassium phosphate buffer (pH 7.0), resuspended with the
 19 same buffer, and sonicated by two 30-s bursts with a Braun-Sonifier 250 apparatus.
 20 After centrifugation for 30 min at 18,000 x g at 4°C, the supernatant was used for the
 21 determination of enzyme activity.

22 **Co-expression of *nbaA* and *nbaB* in *E. coli*.** Two strategies were used. First, tandem
 23 expression of the two genes on a single plasmid, and second, expression of *nbaA* and
 24 *nbaB* on two compatible plasmids. In the tandem gene construct, the strategy was to
 25 have a single transcript producing two independently translated polypeptides with the
 26 use of a strong ribosomal binding site located between the two genes. Toward this

1 construction, a synthetic ribosomal binding site was introduced after NbaA into the
 2 original pSD80.NbaA clone at the HindIII and NheI sites, using the primers
 3 pSD80PC5'
 4 5'-AGCTTTGCACATATCGAGGTGAACATCACGCCCGGGTAAGGAGGTGGCGC
 5 GCCCTCGAGG and pSD80PC3'
 6 5'-CTAGCCTCGAGGGCGCGCCACCTCCTTACCCGGGCGTGATGTTACCTCG
 7 ATATGTGCAA, producing pSD80.NbaA.SD. The synthetic region contains the
 8 ribosomal binding sequence as well as the restriction endonuclease sites for HindIII,
 9 SmaI, AscI, XhoI and NheI. NbaB was amplified from the original pSD80.NbaB
 10 clone using the primers: NbaB5'-AscI
 11 5'-TTGGCGCGCCATGTCCAATGCCCGAATG and pSD80R
 12 5'-GTTTTATCAGACCGCTTCTGCG. The product was ligated into
 13 pSD80.NbaA.SD at AscI and NheI creating the single plasmid clone
 14 pSD80.NbaA.SD.NbaB. The final plasmid was transformed into *E. coli* BL21(DE3)
 15 Rosetta (Novagen) cells containing the pRARE plasmid which encodes rare *E. coli*
 16 tRNA codons resulting in enhanced recombinant protein expression otherwise limited
 17 by codon usage. Ampicillin and chloramphenicol were used for plasmid selection and
 18 maintenance in the same cell. Cells were grown overnight in LB Amp/Cm, subcultured
 19 (1:100) and induced with 1mM IPTG at OD 0.5 for 5 hours.

20 The compatible plasmid system consists of pREP1.SD.NbaA and pT7-5.SD.NbaB
 21 derived from pREP1 and pT7-5, respectively, according to Parales et al (57). As
 22 described above, the synthetic ribosomal binding site was introduced into the pSD80
 23 vector producing pSD80.SD. NbaB was amplified as described above. NbaA was
 24 amplified from the original pSD80.NbaA clone using the primers: NbaA5'-AscI 5'-
 25 TTGGCGCGCCATGACGCACATTGCAATGTCAG and pSD80R. Both NbaA and
 26 NbaB products were introduced into pSD80.SD at the AscI and NheI sites. Both

1 SD.NbaA and SD.NbaB were amplified using the primers pSD80pc5'-SmaI 5'-
2 CACGCCCGGGTAAGGAGG and pSD80 R and cloned into pREP1 and pT7-5
3 respectively, at the SmaI and PstI sites. The plasmids were transformed in
4 JM109(DE3) that has the IPTG-inducible T7 RNA polymerase on the chromosome.
5 Ampicillin and chloramphenicol were used for plasmid selection and maintenance in
6 the same cell. Cells were grown overnight in LB Amp/Cm, subcultured (1:100) and
7 induced with 1mM IPTG at OD 0.5 for 5 hours.

8 1 mM final concentration of 2-NBA was added to the single and double plasmid
9 cultures and grown overnight. The cells were centrifuged and an aliquot (20 μ l) of the
10 supernatant was spotted on TLC plates (Sigma T-6145). Authentic standards of 2-NBA
11 and 3-HAA from Sigma were used to match the R_f values of the substrate and product.
12 TLC was developed with ethyl acetate:hexane (1:1), dried and observed under UV
13 light. 2-NBA appeared purplish and 3-HAA appeared yellow.

14 **Enzyme activities. (i) 2-NBA nitroreductase activity.** 2-NBA nitroreductase
15 activity was measured by monitoring the decrease in absorbance at 340 nm with the
16 conversion of NADPH to NADP⁺ in a spectrophotometer (27). Reaction mixtures
17 contained 2-NBA (0.2 μ mol), NADPH (0.2 μ mol), potassium phosphate buffer (50
18 μ mol, pH 7.0), and appropriate amount of cell-free extracts in a final volume of 1 ml.

19 To identify 2-HABA as a reaction product, 0.25 μ mol of 2-NBA and 0.96 μ mol of
20 NADPH were incubated with a cell-free extract of *E. coli* BL21(pSDnbaA) in 30 mM
21 potassium phosphate buffer (pH7.0) in a total volume of 500 μ l. After 10 min
22 incubation at 30 °C, the reaction mixture was analyzed by HPLC. Control experiments
23 were carried out without the addition of heterologous proteins. One unit (U) of
24 enzyme activity was defined as the quantity of enzyme required to oxidize 1 μ mol
25 NADPH per min. at 25°C. Protein concentrations were determined using the Bradford
26 assay and bovine serum albumin (Pierce, Rockford, Ill) as the protein standard.

1 (ii) **2-HABA mutase activity.** 2-Hydroxyaminobenzoic acid mutase activity was
2 identified by measuring the conversion of 2-HABA to 3-HAA using a preassay
3 mixture that consisted of 0.25 μmol of 2-NBA and 0.96 μmol of NADPH, and
4 cell-free extract of *E. coli* BL21(pSDnbaA) in 30 mM potassium phosphate buffer (pH
5 7.0) in a total volume of 500 μl . The reaction mixture was incubated for 10 min at
6 30°C; an aliquot of *E. coli* BL21(pSDnbaB) cell-free extract was then added and the
7 reaction mixture further incubated for 10 min before analysis by HPLC. One unit (U)
8 of activity is defined as the amount of enzyme required to convert 1 μmol of substrate
9 in 1 min.

10 **HPLC analysis.** A Shimadzu instrument (model LC-6AD) equipped with an UV
11 detector operating at a wavelength of 254 nm was used. Separations were performed
12 on a CAPCELL PAK C18 UG120 column (column size, 4.6 \times 250 mm; particle size, 5
13 μm ; Shiseido, Tokyo) with a methanol-10 mM KH_2PO_4 mixture [30:70 (v/v)] at a flow
14 rate of 1.0 ml min^{-1} as a solvent.

15 **Site-directed mutagenesis.** PCR overlap extension mutagenesis (29) was used to
16 generate *nbaA* mutants using pSDnbaA as template (Table 1). The following 27-mer
17 primers were used and in each case, its complementary mutagenic primer (not shown);
18 the underlined codon represents the alanine (A) change.

19 N40A: 5'-GAGGGGTTGTGCGCGGCCGCGCCTTAT;

20 H63A: 5'-ATCGCCGTGGATGCGTATGGTGAAGAA;

21 H69A: 5'-GGTGAAGAAAGCGCGCGTCCTGGCGAG;

22 D76A: 5'-GGCGAGCAAAAAGCGGACGCTAAAAAAC;

23 H110A: 5'-GATTTCCCCTCTGCGGATCTCAGAAGCC;

24 E113A: 5'-TCTCATATCTCAGCGGCCGAAGCCGTT.

25 After cloning, the sequences of the cloned fragments were confirmed by DNA
26 sequencing and their expression verified.

1 **Partial purification of 2-NBA nitroreductase.** The cell extract of strain KU-7
2 harvested from 1.25 litres of culture was used as the starting material for the
3 purification of 2-NBA nitroreductase. All procedures were carried out at 4°C. The cell
4 extract was fractionated using ammonium sulfate at 30 to 50% saturation. The
5 resulting precipitate was dissolved in 50 mM potassium phosphate buffer (pH 7.0).
6 This enzyme solution was dialyzed against the same buffer for 12 hrs. The dialyzed
7 solution was put on a DEAE-Cellulose DE52 column. The column was washed with
8 50 mM potassium phosphate buffer (pH 7.0) until no protein could be detected in the
9 flow-through, and the enzyme was subsequently eluted with a linear gradient of 0 to
10 0.5 M KCl in the same buffer. Active fractions were collected, pooled, and used as a
11 partially purified 2-NBA nitroreductase.

12 **Protein analysis.** The partially purified 2-NBA nitroreductase was subjected to
13 (12%) sodium dodecyl sulfate-polyacrylamide gel electrophoresis (SDS-PAGE)
14 carried out by conventional method on a Mini-PROTEAN II Electrophoresis cell
15 (Nippon Bio-Rad Laboratories, Tokyo). The gel was transferred to a polyvinylidene
16 difluoride membrane (MiniProBlott; Applied Biosystems Japan Ltd.) with a Mini
17 Trans-Blot electrophoretic transfer cell (Nippon Bio-Rad laboratories) as described by
18 the manufacturer. The area on the membrane containing 2-NBA nitroreductase was cut
19 out and subjected to N-terminal amino acid sequencing with a model PPSQ-21 protein
20 sequencer (Shimadzu Co., Kyoto, Japan).

21 **Molecular modeling of NbaA and its complexes with Ni²⁺, FMN and NADPH.**

22 Structural bioinformatics analysis of the NbaA sequence was carried out at the
23 BioInfoBank MetaServer (<http://bioinfo.pl/meta>), which assembles state-of-the-art
24 fold recognition methods and provides a consensus sequence-to-structure
25 hyper-scoring with the 3D-JURY meta-predictor (24).

26 Structural manipulations were done with the SYBYL 6.6 software (Tripos, Inc., St.

1 Louis, MO). The homology modeling program COMPOSER (7) in SYBYL was
2 employed to delineate six structurally conserved regions (SCRs) and five intervening
3 structurally variable loop regions (SVRs) between NbaA and its template structures.
4 The NbaA residues in the SCRs were modeled based on the structures of the two
5 closest homologs (an FMN-binding protein and a styrene monooxygenase, PDB codes
6 1EJE and 1USF, respectively), while the SVRs were initially built using the PROTEIN
7 LOOPS structure database search module in SYBYL. Based on the crystal structure of
8 the closest NbaA homolog identified (PDB code 1EJE), the NbaA homodimer was
9 then assembled, together with one FMN molecule, one divalent metal ion (Ni^{2+}) and
10 seven adjacent structured water molecules per each monomer. Side chain repacking
11 and re-orientation of polar hydrogens were performed to alleviate minor steric clashes
12 and improve hydrogen bonding. The NbaA- Ni^{2+} -FMN dimeric model was refined by
13 sequential runs of molecular mechanics force field energy minimization that allowed
14 gradual relaxation of (i) the SVRs, (ii) the 23-residue N-terminal segments, and (iii)
15 all side chains.

16 In order to dock NADPH into the modeled NbaA- Ni^{2+} -FMN complex, the
17 nicotinamide mononucleotide (NMN) half of NADPH was manually positioned into
18 its putative binding cleft on NbaA and facing the isoalloxazine ring of FMN, in an
19 orientation and conformation observed in one of the identified NbaA templates (a
20 ferric reductase) complexed with FMN and NADP^+ (PDB code 1IOS). The initial
21 conformation of the 2'-P-AMP half of the NADPH was also built by analogy as
22 extending outward from the pocket. The resulting NADPH binding mode was then
23 relaxed by energy minimization. Feasible bound conformations of the solvent exposed
24 2'-P-AMP moiety were subsequently explored using the Monte Carlo-minimization
25 (MCM) conformational sampling procedure (44) adapted to flexible ligand docking
26 (13, 46, 65). The NMN half of NADPH was kept as an anchor from which random

1 dihedral angle perturbations were introduced in the 2'-P-AMP half of NADPH,
2 followed by energy minimizations, for a total of 10,000 MCM cycles.

3 **Docking of 2-NBA to the modeled NbaA-Ni²⁺-FMN complex.** This was
4 performed manually, first by positioning its aromatic ring similarly with the
5 nicotinamide ring in the modeled NADPH complex (resulting in parallel stacking
6 between 2-NBA and the isoalloxazine ring of FMN). Several alternate orientations of
7 2-NBA with respect to its two *ortho* groups were then generated and refined
8 independently by energy minimization.

9 All conjugate gradient energy minimizations were carried using the AMBER
10 all-atom molecular mechanics force field (17, 73). A distance dependent ($4R_{ij}$)
11 dielectric, an 8 Å non-bonded cutoff and a root-mean-square gradient of 0.05
12 kcal/(mol·Å) were used. The protonation state at physiological pH was adopted.
13 Published AMBER-compatible atomic parameters were used for FMN (46) and
14 NADPH (61). Partial atomic charges for 2-NBA were obtained by a two-stage
15 restrained fitting procedure to the single-point HF 6-31G* electrostatic potential (6)
16 calculated in GAMESS (64). A charge-delocalized model with octahedral geometry
17 was used for Ni²⁺ (55, 65). During all energy minimizations, the FMN and Ni²⁺, as
18 well as the SCR backbone atoms of NbaA were constrained to their initial positions
19 using harmonic potentials with force constants of 20 kcal/(mol·Å²) and 1
20 kcal/(mol·Å²), respectively.

21 **Chemotaxis assay.** The chemotactic behavior of strain KU-7 and its *nbaY* deletion
22 mutant *nbaΔY* was studied by swarm plate assay (26), drop assay (21) and agarose
23 plug assay (41, 75). In the swarm plate assay, soft agar swarm plates consisted of MS
24 medium that contains 1 mM of chemicals (2-NBA, 3-HAA, benzoate, succinate) and
25 0.3% agar. Cells (OD₆₀₀ 1.0) were inoculated at the center of the plates and these
26 plates were incubated at 30°C overnight. The medium used for the drop assay

1 consisted of 50 mM phosphate buffer (pH 7.0) that contains 20 μ M EDTA and 0.05%
2 glycerol. Cells were grown in MS medium, pelleted, washed and suspended in drop
3 assay medium, and finally poured into petri plates. The chemotactic response was
4 determined by placing the paper disk containing 100 mM attractant at the center of the
5 plate. Agarose plug assays were carried out with slight modifications as previously
6 described (41, 75). Plugs contained 2% agarose in chemotaxis buffer (50 mM
7 phosphate buffer (pH 7.0) that contains 20 mM EDTA and 0.05% glycerol), and 10
8 mM 2-NBA. A drop (100 μ l) of the melted agarose mixture was placed on a Petri dish.
9 Cells were grown in MS medium, pelleted, washed and suspended in chemotaxis
10 buffer, and finally poured into Petri plates with agarose plug. The chemotactic
11 response was determined by the ring appearance after 20 min incubation at room
12 temperature.

13 **Nucleotide sequence accession number.** The nucleotide sequence determined in this
14 study has been deposited in the DDBJ under accession number AB263093.

RESULTS AND DISCUSSION

Isolation of the *nbaA* disrupted mutant strain by transposon mutagenesis. In our previous study, analysis of a 19-kb DNA region of strain KU-7 that encompasses the 3-HAA *meta*-cleavage and regulatory gene cluster, designated *nbaEXHJIGFCDR*, was found to be devoid of the two initial degradative genes, *nbaA* and *nbaB* (49). We screened additional Tn5-3/1Tp transformants and obtained apparently new candidates that were unable to grow on 2-NBA as a sole carbon source. Some 500-bp sequences were determined from each IPCR product and used to search the nonredundant protein sequence database of the NCBI for the presence of possible target sequences. However, the majority of the transposon insertion sites, except KUM-9, -19 and -33 (Fig. 1), appeared to bombard the known 3-HAA *meta*-cleavage and regulatory gene cluster (49).

Insertion site of Tn5-3/1Tp in strain KUM-9 was found to be within a 386-codon ORF (Orf16) predicted to encode an ABC transporter substrate binding protein. Its closest homolog (81.8% sequence identity) is a putative extracellular ligand-binding receptor of *Polaromonas* sp. JS666 [CP000317 (ABE46993)]. Tn5-3/1Tp insertion site in strain KUM-19 was found within a sequence, designated Orf23, and subsequently identified as NbaA, that is similar to a FMN-binding protein of *Methanobacterium thermoautotrophicum* Δ H (14). Resting cells of strain KUM-19, grown on succinate as the carbon source that were non-induced with the substrate, did not degrade 2-NBA.

Insertion of the Tn5-3/1Tp transposon into strain KUM-19 was verified by Southern blot analysis of the total DNA digested with *EcoRI* and *BamHI*. As a result, only one hybridization band (a 7.4-kb *EcoRI* fragment and a 4.1-kb *BamHI* fragment) was observed in each digest (Fig. 1).

Cloning and sequencing of the Tn5-3/1Tp flanking regions. Cloning of the 7.4-kb *EcoRI* fragment or the 4.1-kb *BamHI* fragment was carried out by using a pUC19 as a

1 vector. In the former case, transformants were selected on trimethoprim- and
2 ampicillin-containing plates. In the latter case, kanamycin and ampicillin were used as
3 the selection markers. The resulting plasmids were designated pNBA5 and pNBA6,
4 respectively. The pNBA5 insert contained a 4.5-kb Tn5-3/Tp segment and 2.9-kb of
5 KU-7 DNA. Plasmid pNBA6 was found to contain a 3-kb Tn5-3/Tp insert and 1.1 kb
6 of KU-7 DNA.

7 In parallel with the transposon mutagenesis experiment, DNA sequence of the
8 flanking region of the 9.3-kb *Hind*III fragment was determined by direct sequencing
9 of a IPCR product. The template for IPCR was prepared from self-ligated 5.5-kb *Pst*I
10 fragment. The sequence of IPCR product revealed that there is a 13-bp gap between
11 KU-7 DNA in pNBA6 and 9.3-kb *Hind*III fragment (pNBA3).

12 Sequencing of the Tn5-3/Tp flanking regions in pNBA5 and pNBA6 and data
13 analysis revealed three ORFs, two divergently transcribed *orf22* and *orf23*, separated
14 by a 419-bp intergenic space, and 160-bp downstream of *orf23* and on the same DNA
15 strand, the presence of *orf24* (Fig. 1). Various evidence establishing these ORFs as
16 NbaA-, NbaB- and a chemotactic receptor NbaY-encoding genes are provided in the
17 following sections.

18 **Identification of NbaA as 2-NBA nitroreductase.** Sequence determination of the
19 N-terminal 15-amino acid peptide (THIAMSGLTNMQKYW) derived from a partially
20 purified 2-NBA nitroreductase of strain KU-7 confirmed the gene assignment of the
21 651-bp *orf23* that encodes a 216-residue polypeptide that is preceded by an
22 appropriate ribosome-binding sequence (GGAG) 6-bp from the methionine start codon.
23 The predicted molecular size of the protein, M_r of 24,410 matched well with the
24 experimental value of 28 kDa that was derived from a SDS-PAGE of the
25 IPTG-inducible expression of the NbaA protein in pSD*nbaA* (Fig. 2). By SuperdexTM
26 200 gel chromatography, NbaA was found in an active fraction that eluted at a

1 molecular mass that is slightly greater than 44-kDa of molecular standard chicken
2 albumin, indicating NbaA functions as a dimer (not shown).

3 The BLAST search retrieved a number of homologs of microbial origin displaying
4 40-78% sequence identity, but all are hypothetical or uncharacterized proteins. Two
5 such sequences are derived from pollutant-degrading bacteria: a hypothetical
6 conserved protein (77.7% identity), designated [CP000317 (ABE46991)], derived
7 from a large plasmid of *Polaromonas* strain JS666, a chlorinated-alkene-degrading
8 organism; the other, Bcep 4121 (39.7%) derived from a well-known PCB-degrader
9 *Burkholderia xenovorans* (formerly *fungorum*) strain LB400. However, the most
10 useful information comes from a number of structural homologs (presented in a
11 following section), notably an FMN-binding protein (MTH152; accession no.
12 NP_275295, 31 % identity), derived from *Methanobacterium thermoautotrophicum*
13 ΔH (14).

14 **Biochemical properties of NbaA.** The specific activity of NbaA toward 2-NBA was
15 found to be 10.26 U/mg. Crude cell extracts of *E. coli* BL21(pSDnbaA) were able to
16 oxidize NADPH only in the presence of 2-NBA. An investigation of the reaction
17 stoichiometry demonstrated that complete disappearance of 2-NBA by the cell extracts
18 required 2 mol of NADPH per mol of 2-NBA. By HPLC analysis of the NbaA reaction
19 product with 2-NBA and NADPH as substrates, only one product was formed in
20 significant amount with a retention time at 4.96 min. The expected product 2-HABA
21 was identified by comparison to an authentic standard (Fig. 3).

22 Supplements of flavins (FMN, FAD and riboflavin) to crude extracts of *E. coli*
23 BL21(pSDnbaA) at the final concentration of 1.0 mM resulted in an increase of
24 specific activities by 3.8-fold and 5.2-fold in the case of FAD and FMN, respectively.
25 The addition of riboflavin gave the same basal level as the case without the addition of
26 FAD or FMN. Evidently, FMN was more effective than FAD suggesting that FMN

1 may be a physiological cofactor of NbaA.

2 The effect of divalent cations on NbaA activity were examined by preincubating the
3 cell-free extracts containing NbaA with the chloride salts of the divalent cations: Ca,
4 Co, Cu, Fe, Mg, Mn, Ni and Zn, at 0.1 mM and 0.3 mM. Fe, Mg and Mn appeared to
5 have a potentiating effect at 0.1 mM providing a 23%, 16% and 51% increase in
6 activity, respectively. The addition of 0.3 mM Fe²⁺ and Mn²⁺ gave the most increase,
7 66% and 89%, respectively, whereas, Ni²⁺ showed an increase of 17%. Ca²⁺ and Zn²⁺
8 seem to inhibit the enzyme to some extent. Under these experimental conditions, Mn²⁺
9 rendered the best activity to NbaA.

10 **Modeled NbaA structure and interactions.** Structural bioinformatics searches
11 unambiguously assigned the NbaA protein to the FMN-binding split barrel fold, and
12 specifically to the NADH:FMN oxidoreductase-like structural family (accession
13 numbers b.45.1.2 or 50482) according to the SCOP database
14 (<http://scop.berkeley.edu/>) (3), also classified as the flavin reductase-like domain
15 (accession number PF01613) in the Pfam database
16 (<http://www.sanger.ac.uk/Software/Pfam/>) (4). Currently, the solved structures
17 adopting this fold include the FMN-binding protein MTH152 from *M.*
18 *thermoautotrophicum* (PDB code 1EJE) (14), a ferric reductase from *Archeoglobus*
19 *fulgidus* (PDB codes 1I0R and 1I0S) (12), the flavin reductase PheA2 from *Bacillus*
20 *thermoglucosidasius* (PDB codes 1RZ0 and 1RZ1) (70), a styrene monooxygenase
21 from *Thermus thermophilus* (PDB codes 1USC and 1USF) (unpublished), and a
22 probable flavoprotein from the same organism (PDB codes 1WGB and 1YOA)
23 (unpublished). The sequence alignment of NbaA and these five structurally similar
24 enzymes is given in Fig. 4A.

25 This alignment formed the basis for the three-dimensional homology modeling of
26 the NbaA homodimeric structure (Fig. 4B). The core of each modeled NbaA subunit is

1 proposed to be organized around a six-stranded antiparallel β -barrel with a capping
2 α -helix, a fold recognized as a circular permutation of the flavin binding domain of
3 the ferredoxin reductase superfamily (34, 45, 50). However, the ferredoxin
4 reductase-type proteins utilize a second, Rossmann fold domain to bind the NAD(P)H
5 (34). The homology to the NADH:FMN oxidoreductase-like fold family strongly
6 suggests that the predicted single-domain structure of NbaA would provide both the
7 flavin and NAD(P)H binding sites (12, 70).

8 The modeled binding mode of FMN to NbaA (Fig. 4C) is similar to that observed in
9 other members of the NADH:FMN oxidoreductase-like fold family (12, 70). FMN fits
10 into a well-shaped groove near the homodimer interface of NbaA. Based on this
11 proposed model, the *si* face of the isoalloxazine ring is buried against the β -barrel and
12 directly contacts the main-chain atoms of residues Ser45, Ala46, Ala60, Asp62, and
13 side-chain atoms of Ser45 and Lys75 *via* hydrogen bonds, as well as Ile27, Pro43,
14 Tyr44, Met100, Val101, Arg187 and Tyr193 by non-polar contacts. The 3'-hydroxyl
15 group of the ribityl moiety is modeled in hydrogen bond contact with the Lys75 side
16 chain. The FMN phosphate group is predicted to be anchored to the β -barrel-capping
17 α -helix of NbaA *via* hydrogen bonds to the Asn40, Tyr44 and Thr77 side chains and to
18 Asp76 and Thr77 main-chain atoms.

19 A divalent metal ion, Ni^{2+} , was modeled as mediating the interaction between the
20 FMN phosphate and NbaA. This interaction has been observed in the crystal structure
21 of the FMN-binding protein MTH152 (PDB code 1EJE) (14), the structural template
22 most similar in primary sequence to NbaA. In the more distant structural homologs of
23 NbaA, this phosphate-bridging role is fulfilled by protein side chains, e.g., the
24 ammonium group of Lys69 in ferric reductase (PDB codes 1I0R and 1I0S) (12). In the
25 modeled NbaA-FMN complex, the octahedral coordination sphere of the Ni^{2+} metal
26 ion consists of side-chain oxygen atoms from residues Asn40, Asp76 and Glu113

1 (Asn36, His62 and Glu99, respectively, in the FMN-binding protein MTH152), two
2 water molecules, and an oxygen atom from the FMN phosphate (Fig. 4C).

3 The NADPH binding mode to NbaA (Fig. 4D) was inferred from the NADP⁺
4 binding mode observed in some of the structural homologs (styrene monooxygenase,
5 ferric reductase and flavin reductase PheA2, PDB codes 1USF, 1IOS and 1RZ1,
6 respectively), primarily for the more buried NMN half of NADPH. In this binding
7 mode, the nicotinamide ring stacks against the available *re* face of the FMN
8 isoalloxazine ring. The modeled C4(nicotinamide)-N5(isoalloxazine) distance of
9 ~3.5 Å is compatible with a direct hydride transfer from NADPH to FMN (12, 70).
10 The amide group of nicotinamide is predicted to form hydrogen bonds with the side
11 chains of Asp62, Arg153, as well as Tyr49 from the second subunit in the NbaA
12 homodimer. In this plausible model, the NMN phosphate would be stabilized by a
13 salt-bridge with Arg187.

14 Multiple sterically feasible binding modes may be expected for the solvent exposed
15 2'-P-AMP fragment of NADPH, due to the fairly wide opening at the top of the FMN
16 and NMN binding cleft of NbaA. Although the low-energy conformations obtained
17 from conformational sampling indeed revealed variability in the binding mode of the
18 adenosine portion of NADPH, it also appeared that the adenine moiety has a tendency
19 to interact with the loop $\beta 5$ - $\alpha 2$ of NbaA (Fig.4B, 4D). The resolution of our modeled
20 structure in this solvent exposed region does not allow speculations on specific
21 intermolecular interactions. Interestingly, the $\beta 5$ - $\alpha 2$ loop of NbaA includes a
22 10-residue insertion relative to the other members of the NADH:FMN
23 oxidoreductase-like structural family (Fig. 4A). Thus, it resembles the corresponding
24 loop of the ferredoxin reductase superfamily members, that has been shown to be able
25 to interact *via* one of its aromatic residues with the adenine moiety of FAD (8, 19).
26 The $\beta 5$ - $\alpha 2$ loop of NbaA does include an aromatic residue, His69, which might

1 therefore represent a potential site for interaction with the adenine moiety of NADPH.

2 **Proposed NbaA reaction mechanism.** A structural model for the 2-NBA substrate
3 binding mode to NbaA assumes the ping-pong mechanism in which the oxidized
4 coenzyme leaves its binding site and is replaced by the substrate that contacts the
5 enzyme-bound reduced flavin. This assumption is supported by the available data for
6 NbaA structural homologs such as ferric reductase (12) and flavin reductase PheA2
7 (71), where steric constraints impede simultaneous binding of the substrate and
8 nicotinamide, thus suggesting a ping-pong kinetic mechanism. Indeed, biochemical
9 data have recently shown that the flavin reductase PheA2 catalyzes the
10 NADH-dependent reduction of free flavins by a ping-pong bisubstrate-biproduct
11 mechanism (36). [Other nitroaromatic reductases, although not displaying significant
12 sequence or structural similarities to NbaA, have been shown to act according to a
13 ping-pong catalytic mechanism.](#) For example, the structures of nitroaromatic
14 reductases from *E. coli* and *Enterobacter cloacae* complexed with substrate analogs,
15 inhibitors and dinitrobenzoate prodrugs show that these ligands replace the NAD(P)H
16 nicotinamide in order to form parallel stacking with the isoalloxazine moiety of
17 enzyme-bound FMN or FMNH₂ (28, 33, 48). Furthermore, a recent kinetic study of *E.*
18 *coli* nitroaromatic reductase demonstrates that the nitroso-intermediate becomes the
19 substrate in a subsequent enzyme-catalyzed reduction reaction leading to the
20 hydroxylamine product (59). A plausible ping-pong mechanism for reaction catalyzed
21 by NbaA is depicted in Fig. 5.

22 Our model of 2-NBA bound to NbaA (Fig. 4E) is consistent with the observed
23 orientation of the substrate nitrophenyl moiety against the nitroreductase-bound flavin
24 (33). According to this putative binding mode, the aromatic substrate forms a parallel
25 stacking with the isoalloxazine ring. The nitro group of 2-NBA would contact the
26 isoalloxazine rings above the N5 nitrogen atom, where it is predicted to be anchored

1 by polar interactions with the Arg25 and Arg187 positively charged side chains of
2 NbaA. These interactions remain compatible with the binding of the 2-nitrosobenzoate
3 intermediate, but not with the 2-hydroxyaminobenzoate product, due to electrostatic
4 repulsions between positively charged hydrogen atoms. In the proposed model, the
5 *ortho* carboxylate substituent of 2-NBA is complementary to its putative binding site
6 on NbaA by forming a salt-bridge with the side chain of Arg153, and hydrogen bonds
7 with Thr19 and Tyr49 (from the second monomer), which may account for the NbaA
8 specificity toward 2-NBA. For example, a similar carboxylate binding motif (i.e., Arg,
9 Ser, Tyr) is present in *p*-hydroxybenzoate hydroxylase (65).

10 **Site directed mutagenesis of predicted NbaA active site residues.** Structural
11 modeling analysis of relevant NbaA complexes suggests how specific residues may
12 contribute to the catalytic activity of the enzyme, and thus forms the basis for
13 mutational analyses. We first probed by site-directed mutagenesis the predicted metal
14 binding residues Asn40, Asp76 and Glu113. We also mutated residue His69 from the
15 10-residue insertion loop β 5- α 2 predicted to interact with the adenosine portion of
16 NAD(P)H. Mutations of two other histidine residues, His63 and His110, predicted to
17 be solvent exposed and not to contribute to NbaA activity (neither *via* ligand binding
18 nor dimerization), were also tested. Hence, we generated six NbaA variants that in
19 each case resulted in an alanine substitution. Individual mutations of the three
20 predicted divalent metal ion binding site residues (N40A, D76A, and E113A) resulted
21 in a complete loss of the NbaA activity (Table 2). These results are in agreement with
22 our model showing that the metal ion would act as a bridge between the FMN
23 phosphate and the protein, thus being essential for FMN binding (Fig. 4C). The H69A
24 substitution resulted in an enzyme that retained only 2-3% of the wild-type NbaA
25 activity, but nonetheless still active (Table 2). In a recent study of another
26 NADH:flavin oxidoreductase, a similar drop in activity has been observed for a

1 histidine residue that represents an NADH interacting site (60). Taken together, these
2 observations are in agreement with the predicted NAD(P)H interacting role of His69
3 in NbaA. On the other hand, the H63A and H110A substitutions retained 72-73% and
4 33-44% of the original activity, respectively, indicating that these residues do not
5 contribute substantially toward NbaA activity. For all active mutants, it was shown
6 that the addition of exogenous FMN potentiated the various enzyme activities about 3
7 to 5 fold. We also noted that the amounts of the variant NbaA proteins produced, as
8 evident in a Coomassie-stained SDS-PAGE analysis, are comparable to the native
9 NbaA (results not shown). Certainly, additional biochemical data from purified
10 enzyme and direct experimental structural evidence will be required for a refined
11 characterization of the NbaA catalytic residues and mechanism.

12 **Identification of NbaB as 2-hydroxylaminobenzoate mutase.** The deduced
13 181-amino acid sequence of NbaB showed 35% identity to the
14 4-hydroxylaminobenzoate lyase (PnbB) sequences of three known degradative
15 organisms - *P. putida* TW3 degrading 4-nitrotoluene (31), and *Pseudomonas* sp.
16 YH102 and *Ralstonia pickettii* YH105, degrading 4-nitrobenzoate (76). Higher
17 identities were observed with four hypothetical proteins in the genomes of *Rhodofera*
18 *ferrireducens* DSM 15236 (38%); *Azoarcus* sp. EbN1 (39.3%), *Burkholderia*
19 *fungorum* LB400 (40%), and *Polaromonas* sp. JS666 (66.5%). A multiple sequence
20 alignment of the PnbB lyases with NbaB (Supplemental Fig. S2) revealed that the
21 conserved sequences are distributed evenly throughout the polypeptide with the
22 exception that NbaB (and its JS666 homolog) appears to have an N-terminal extension
23 of 14-20 residues and two sequence gaps (amino acids 110-111 and 142-143 [NbaB
24 numbering]) are needed for an optimal sequence alignment. The sequence similarity
25 between PnbB and NbaB provides a plausible basis for the second action of PnbB in
26 the 4-nitrobenzoate pathway of *P. putida* strain TW3 in the production of

1 4-amino-3-hydroxybenzoate from 4-nitrobenzoate besides the better known product,
2 protocatechuate (31). Evidently, 4-amino-3-hydroxybenzoate is an analog of
3 2-amino-3-hydroxybenzoate, i.e. 3-HAA.

4 The expression of a 22-kDa protein band, although weak, derived from plasmid
5 pSDnbaB confirmed the expected molecular mass of NbaB, calculated to be 19,554
6 (Fig. 2). No enhanced protein band of this size was detectable in the control cells
7 containing the pSD80 vector only. However, a better expression of NbaB was seen in
8 the pT7-5SD.NbaB construct transformed in *E. coli* JM109(DE3) (Fig. 2). This level
9 was just as good as the expression of NbaA in pSDnbaA. On the other hand, NbaA was
10 not readily expressed in the pREP1.NbaA construct as in pSDnbaA.

11 By HPLC analysis of the enzyme reaction product of NbaB with 2-NBA and
12 NADPH in the presence of NbaA, the reaction product, a peak at retention time 4.40
13 min, was identified to be 3-HAA, by comparison to an authentic standard (Fig. 3).
14 3-HAA production by the appearance of a yellow spot under UV illumination was also
15 observed by thin layer chromatography (not shown).

16 **NbaY (Orf24) gene disruption and chemotaxis.** This Orf24 consists of sequence
17 coding for 544 amino acid residues. The primary structure showed 29% sequence
18 identity to NahY from *P. putida* G7, a known methyl-accepting chemotactic transducer
19 that recognizes naphthalene (25). An updated BLAST search showed 62-63%
20 sequence homology to a putative chemotaxis sensory transducer, [CP000094
21 (ABA74342)] and [CP000076 (AAY92385)], each derived from *P. fluorescens* strains
22 PfO-1 and Pf-5, respectively. A multiple sequence alignment is shown in
23 Supplemental Fig. S3. The greatest sequence conservation occurs within a region
24 designated the HCD, highly conserved domain, typical of chemoreceptor proteins (39).
25 In NbaY, two possible transmembrane segments (amino acids 13-35 and 190-212 are
26 predicted.

1 To test whether NbaY serves as a possible chemoreceptor for 2-NBA, we
2 constructed a *nbaY* deletion mutant, designated strain KU- Δ Y. The use of three
3 independent assays by their ring appearance in the case of the wildtype compared to
4 the mutant supported the involvement of NbaY in 2-NBA chemotaxis (Fig. 6). In
5 liquid culture, strain KU- Δ Y grew just as readily as the wildtype when 2-NBA was
6 used as the sole carbon source. At this time, we have not tested whether any of the
7 2-NBA metabolite would serve as a chemoattractant. A detailed chemotaxis study is
8 outside our present scope.

9 To the best of available knowledge, NahY and PcaK (a transporter and
10 chemoreceptor protein from *P. putida* PRS2000 that is encoded as part of the
11 beta-ketoadipate pathway regulon for aromatic acid degradation) are two of the
12 existing characterized chemoreceptor genes for aromatic metabolism (reviewed in
13 54, 58). On the other hand, there have been several studies illustrating chemotaxis
14 of a variety of nitroaromatic degradative organisms toward compounds such as
15 nitrotoluene, dinitrotoluene, and TNT etc. (43, 54, 56, 58). But in all cases, no
16 pathway-associated gene, like NahY in naphthalene degradation, PcaK in benzoate
17 metabolism or NbaY as in this study, has been ascribed to the observed chemotaxis
18 phenomena. Hence, NbaY is a prototype chemoreceptor for nitroaromatics. The
19 relevance of chemotaxis in pollutant-degrading bacteria to bioremediation strategy
20 has been reviewed (54, 58).

21 **Concluding remarks.** For the first time, a homology model of 2-nitrobenzoate
22 nitroreductase is available that adds to our limited knowledge on structure and
23 function of nitroreductases in nitroaromatic metabolism of which a limited number of
24 genetic and/or biochemical studies are available (11, 35, 40, 51, 67). NbaA is a new
25 representative of a family of homodimeric NADH:FMN oxidoreductase-like fold
26 proteins that is different from the nitro/flavin reductase family. The latter comprises of

1 the major oxygen-insensitive nitroreductase (NfsA) from *E. coli* NfsA (37), flavin
2 reductase (FRP) of *Vibrio harveyi* (42), PnrA of a TNT-degrading *P. putida* JLR11 (11),
3 and NitA and NitB of another TNT-degrading *Clostridium acetobutylicum* ATCC 824
4 (40). It remains to be seen whether the 10-residue insertion loop between strand β 5
5 and helix α 2 (amino acids 65-74) is unique to NbaA that attacks an *ortho*-substituted
6 nitroaromatic substrate. It is unfortunate that we are as yet unable to assign a function
7 or substrate to the MTH152 FMN-binding protein of *M. thermoautotrophicum* (14).
8 However, the structure relationship of MTH152 to NbaA suggests that aromatic
9 compounds should be tested as possible substrates.

10 The availability of NbaA and NbaB-encoding genes paves a plausible
11 biotechnological route for the production of 3-HAA, a known antioxidant and
12 reductant. However, for an efficient substrate uptake of aromatic acid such as
13 2-NBA, this recombinant route might require involvement of the numerous
14 ABC-transporter permease and outer membrane porin sequences, etc., that are
15 possibly encoded by Orfs 16, 14, 13, 12, and 11 (immediately downstream of *nbaB*),
16 and Orf17 that is downstream of the *nbaE* gene cluster (49; DDBJ database accession
17 number AB088043).

18 This study completes the gene elucidation of 2-NBA metabolism in strain KU-7 in a
19 24-kb chromosomal locus, that includes a chemoreceptor gene (*nbaY*) on the 5'-end
20 flanking the core biodegradative gene cluster
21 (*nbaAB[orf]_{16,15,14,13,12,11}nbaEXHJIGFCD*), and a putative transcriptional regulator
22 (*nbaR*) of the LysR-type on the 3'-end that is followed by an unknown *orf17* (49; Fig.
23 7). Interestingly, in the current microbial genome sequence database (JGI database),
24 we have identified the presence of a very similar gene cluster, exhibiting high
25 sequence identities (in the range 63% - 87%), that is encoded on a plasmid of
26 360,405-bp, in the draft genome sequence of *Polaromonas* sp. JS666, a strain studied

1 for its degradation of chlorinated alkenes such as *cis*-dichloroethene, but no other
2 compounds (16). Evidently, the gene organization of the core *nba* biodegradative gene
3 cluster (i.e, from *nbaA* to *nbaR*) is the same in the two strains. Notable differences are
4 in the lengths of the various intergenic spaces and especially the presence of a putative
5 integrase and insertion sequence IS3 and IS911 found at both ends of the JS666 gene
6 locus, in the regions otherwise occupied by *nbaY* and *orf17* in strain KU-7 (Fig. 6).
7 This observation leads to the possibility that the *nba* gene locus constitutes a
8 transferable or transposable “genomic island” or integrative and conjugative elements
9 as frequently found among catabolic pathways of pollutant-degrading bacteria (72).

12 ACKNOWLEDGMENTS

13 We thank A. Nakazawa for providing pKN31 and the National Bioresource Project
14 (National Institute of Genetics, Japan) for plasmid pK18mobsacB. This research was
15 financially supported in part by the Kansai University Research Grants: Grant-in-Aid
16 for Encouragement of Scientists, 2006 (H.I.), and a High-Tech Research Center
17 Project for Private Universities: matching fund subsidy from Ministry of Education,
18 Culture, Sports, Science and Technology, 2002-2006 (Y.H.). We would like to dedicate
19 this paper to the memory of Professor Tai Tokuyama.

22 REFERENCES

- 23 1. Abe, M., M. Tsuda, M. Kimito, S. Inoue, A. Nakazawa, and T. Nakazawa. 1996.
24 A genetic analysis system of *Burkholderia cepacia*: construction of mobilizable
25 transposon and cloning vector. *Gene* 174:191-194.
26 2. Altschul, S. F., T. L. Madden, A. A. Schaffer, J. Zhang, Z. Zhang, W. Miller,

- 1 **and D. J. Lipman.** 1997. Gapped BLAST and PSI-BLAST: a new generation of
2 protein database search programs. *Nucleic Acids Res.* **25**: 3389-3402.
- 3 3. **Andreeva A., D. Howorth, S. E. Brenner, T. J. P. Hubbard, C. Chothia, and A.**
4 **G. Murzin.** 2004. SCOP database in 2004: refinements integrate structure and
5 sequence family data. *Nucleic Acids Res.* **32**:D226-D229.
- 6 4. **Bateman, A., L. Coin, R. Durbin, R. D. Finn, V. Hollich, S. Griffiths-Jones, A.**
7 **Khanna, M. Marshall, S. Moxon, E. L. L. Sonnhammer, D. J. Studholme, C. Yeats,**
8 **and S. R. Eddy.** 2004. The Pfam protein families database. *Nucleic Acids Res.*
9 **32**:D138-D141.
- 10 5. **Bauer, H., and S. M. Rosenthal.** 1944. 4-Hydroxylaminobenzenesulfonamide, its
11 acetyl derivatives and diazotization reaction. *J. Am. Chem. Soc.* **66**:611-614.
- 12 6. **Bayly, C. I., P. Cieplak, W. Cornell, and P. A. Kollman.** 1993. A well-behaved
13 electrostatic potential based method using charge restraints for deriving atomic
14 charges: the RESP model. *J. Phys. Chem.* **97**:10269-10280.
- 15 7. **Blundell, T., D. Carney, S. Gardner, F. Hayes, B. Howlin, T. Hubbard, J.**
16 **Overington, D. A. Singh, B. L. Sibanda, and M. Sutcliffe.** 1988. Knowledge-based
17 protein modelling and design. *Eur. J. Biochem.* **172**:513-520.
- 18 8. **Bruns, C.M., and P.A. Karplus.** 1995. Refined crystal structure of spinach
19 ferredoxin reductase at 1.7 Å resolution: Oxidized, reduced and 2'-phospho-5'-AMP
20 bound states. *J. Mol. Biol.* **247**:125-145.
- 21 9. **Bryant, C., and W. D. McElroy.** 1991. Nitroreductases, p. 291-304. *In* F. Muller
22 (ed.), *Chemistry and biochemistry of flavoenzymes*, vol. II. CRC Press, Boca Raton,
23 Fla.
- 24 10. **Bullock, W. O., J. M. Fernandez, and J. M. Stuart.** 1987. XL-1 Blue: a high
25 efficiency plasmid transforming *recA Escherichia coli* strain with beta-galactosidase
26 selection. *BioTechniques* **5**:376-379.

- 1 11. **Caballero, A., J.J. Lazaro, J.L. Ramos, and A. Esteve-Nunez.** 2005. PnrA, a
2 new nitroreductase-family enzyme in the TNT-degrading strain *Pseudomonas putida*
3 JLR11. *Environ. Microbiol.* **7**:1211-1219.
- 4 12. **Chiu, H., E. Johnson, I. Schroder, and D.C. Rees.** 2001. Crystal structures of a
5 novel ferric reductase from the hyperthermophilic archaeon *Archaeoglobus fulgidus*
6 and its complex with NADP⁺. *Structure.* **9**:311-319.
- 7 13. **Chowdhury, S. F., J. Sivaraman, J. Wang, G. Devanathan, P. Lachance, H. Qi,**
8 **R. Menard, J. Lefebvre, Y. Konishi, M. Cygler, T. Sulea, and E. O. Purisima.** 2002.
9 Design of noncovalent inhibitors of human cathepsin L. From the 96-residue
10 proregion to optimized tripeptides. *J. Med. Chem.* **45**:5321-5329.
- 11 14. **Christendat, D., A. Yee, A. Dharamsi, Y. Kluger, A. Savchenko, J. R. Cort, V.**
12 **Booth, C. D. Mackereth, V. Saridakis, I. Ekiel, G. Kozlov, K. L. Maxwell, N. Wu,**
13 **L. P. McIntosh, K. Gehring, M. A. Kennedy, A. R. Davidson, E. F. Pai1, M.**
14 **Gerstein, A. M. Edwards and C. H. Arrowsmith.** 2000. Structural proteomics of an
15 archaeon. *Nature Struct. Biol.* **7**:903-909.
- 16 15. **Colabroy, K.L., and T.P. Begley.** 2005. Tryptophan catabolism: Identification and
17 characterization of a new degradative pathway. *J. Bacteriol.* **187**:7866-7869.
- 18 16. **Coleman, N.V., T.E. Mattes, J.M. Gossett, and J.C. Spain.** 2002. Biodegradation
19 of *cis*-dichloroethene as the sole carbon source by a beta-proteobacterium. *Appl.*
20 *Environ. Microbiol.* **68**:2726-2730.
- 21 17. **Cornell, W. D., P. Cieplak, C. I. Bayly, I. R. Gould, K. M. Merz Jr., D. M.**
22 **Ferguson, D. C. Spellmeyer, T. Fox, J. W. Caldwell, and P. A. Kollman.** 1995. A
23 second generation force field for the simulation of proteins, nucleic acids, and organic
24 molecules. *J. Am. Chem. Soc.* **117**:5179-5197.
- 25 18. **Dedonder, R.** 1966. Levansucrase from *Bacillus subtilis*. *Methods Enzymol.*
26 **8**:500-505.

- 1 19. Deng, Z., A. Aliverti, G. Zanetti, A. K. Arakaki, J. Ottado, E. G. Orellano, N. B.
2 Calcaterra, E. A. Ceccarelli, N. Carrillo, and P. A. Karplus. 1999. A productive
3 NADP⁺ binding mode of ferredoxin-NADP⁺ reductase revealed by protein
4 engineering and crystallographic studies. *Nat. Struct. Biol.* **6**:847-853.
- 5 20. Esteve-Nunez, A., A. Caballero, and J.L. Ramos. 2001. Biological degradation
6 of 2,4,6-trinitrotoluene. *Microbiol. Mol. Biol. Rev.* **65**:335-352.
- 7 21. Fahrner, K. A., S. M. Block, S. Krishnaswamy, J. S. Parkinson, and H. C.
8 Berg. 1994. A mutant hook-associated protein (HAP3) facilitates torsionally induced
9 transformations of the flagellar filament of *Escherichia coli*. *J. Mol. Biol.*
10 **238**:173-186.
- 11 22. Fath, M., and R. Kolter. 1993. ABC transporters: bacterial exporters. *Microbiol.*
12 *Rev.* **57**:995-1017.
- 13 23. Gay, P., D. Le Coq, M. Steinmetz, T. Berkelman, and C. I. Kado. 1985. Positive
14 selection procedure for entrapment of insertion sequence elements in gram-negative
15 bacteria. *J. Bacteriol.* **164**:918-921.
- 16 24. Ginalski, K., A. Elofsson, D. Fischer, and L. Rychlewski. 2003. 3D-Jury: a
17 simple approach to improve protein structure predictions. *Bioinformatics*
18 **19**:1015-1018.
- 19 25. Grimm, A. C., and C. S. Harwood. 1999. NahY, a catabolic plasmid-encoded
20 receptor required for chemotaxis of *Pseudomonas putida* to the aromatic hydrocarbon
21 naphthalene. *J. Bacteriol.* **181**:3310-3316.
- 22 26. Harwood, C. S., N. N. Nichols, M.-K. Kim, J. L. Ditty, and R. E. Parales. 1994.
23 Identification of the *pcaRKF* gene cluster from *Pseudomonas putida*: involvement in
24 chemotaxis, biodegradation, and transport of 4-hydroxybenzoate. *J. Bacteriol.*
25 **176**:6479-6488.
- 26 27. Hasegawa, Y., T. Muraki, T. Tokuyama, H. Iwaki, M. Tatsuno, and P. C. K.

- 1 **Lau.** 2000. A novel degradative pathway of 2-nitrobenzoate via 3-hydroxyanthranilate
2 in *Pseudomonas fluorescens* strain KU-7. FEMS Microbiol. Lett. **190**:185-190.
- 3 28. **Haynes, C. A., R. L. Koder, A-F. Miller, and D. W. Rodgers.** 2002. Structures of
4 nitroreductase in three states. J. Biol. Chem. **277**:11513-11520.
- 5 29. **Horton, R. M.** 1995. PCR-mediated recombination and mutagenesis. SOEing
6 together tailor-made genes. Mol. Biotechnol. **3**:93-99.
- 7 30. **Huang, G., L. Zhang, and R. G. Birch.** 2000. Rapid amplification and cloning of
8 Tn5 flanking fragments by inverse PCR. Lett. Appl. Microbiol. **31**:149-153.
- 9 31. **Hughes, M. A., M. J. Baggs, J. Al-Dulayymi, M. S. Baird, and P. A. Williams.**
10 2002. Accumulation of 2-aminophenoxazin-3-one-7-carboxylate during growth of
11 *Pseudomonas putida* TW3 on 4-nitro-substituted substrates requires
12 4-hydroxylaminobenzoate lyase (PnbB). Appl. Environ. Microbiol. **68**:4965-4970.
- 13 32. **Hughes, M. A., and P. A. Williams.** 2001. Cloning and characterization of the *pnb*
14 genes, encoding enzymes for 4-nitrobenzoate catabolism in *Pseudomonas putida* TW3.
15 J. Bacteriol. **183**:1225-1232.
- 16 33. **Johansson, E, G. N. Parkinson, W. A. Denny, and S. Neidle.** 2003. Studies on
17 the nitroreductase prodrug-activating system. Crystal structures of complexes with the
18 inhibitor dicoumarol and dinitrobenzamide prodrugs and of the enzyme active form. J.
19 Med. Chem. **46**:4009-4020.
- 20 34. **Karplus, P. A., M. J. Daniels, and J. R. Herriott.** 1991. Atomic structure of
21 ferredoxin-NADP+ reductase: prototype for a structurally novel flavoenzyme family.
22 Science **251**:60-66.
- 23 35. **Kim, H.-Y., and H.-G. Song** 2005. Purification and characterization of
24 NAD(P)H-dependent nitroreductase I from *Klebsiella* sp. C1 and enzymatic
25 transformation of 2,4,6-trinitrotoluene. Appl. Microbiol. Biotechnol. **68**:766-773.
- 26 36. **Kirchner, U., A. H. Westphal, R. Muller, and W. J. van Berkel.** 2003. Phenol

- 1 hydroxylase from *Bacillus thermoglucosidasius* A7, a two-protein component
2 monooxygenase with a dual role for FAD. J. Biol. Chem. **278**: 47545-47553.
- 3 37. **Kobori, T., H. Sasaki, W.C. Lee, S. Zenno, K. Saigo, M.E.P. Murphy, and M.**
4 **Tanokura.** 2001. Structure and site-directed mutagenesis of a flavoprotein from
5 *Escherichia coli* that reduces nitrocompounds. J. Biol. Chem. **276**:2816-2823.
- 6 38. **Krogh, A., B. Larsson, G. von Heijne, and E. L. L. Sonnhammer.** 2001.
7 Predicting transmembrane protein topology with a hidden Markov model: Application
8 to complete genomes. J. Mol. Biol. **305**:567-580.
- 9 39. **Kuroda, A., T. Kumano, K. Taguchi, T. Nikata, J. Kato, and H. Ohtake.** 1995.
10 Molecular cloning and characterization of a chemotactic transducer gene in
11 *Pseudomonas aeruginosa*. J. Bacteriol. **177**: 7019-7025.
- 12 40. **Kutty, R., and G.N. Bennett.** 2005. Biochemical characterization of
13 trinitrotoluene transforming oxygen-insensitive nitroreductases from *Clostridium*
14 *acetobutylicum* ATCC 824. Arch. Microbiol. **184**:158-167.
- 15 41. **Lanfrancini, M. P., H. M. Alvarez, and C. A. Studdert.** 2003. A strain isolated from
16 gas oil-contaminated soil displays chemotaxis towards gas oil and hexadecane.
17 Environ Microbiol **5**:1002-1008.
- 18 42. **Lei, B., M. Liu, S. Huang, and S.-C. Tu.** 1994. *Vibrio harveyi* NADPH-flavin
19 oxidoreductase: cloning, sequencing and overexpression of the gene and purification
20 and characterization of the cloned enzyme. J. Bacteriol. **176**:3536-3543.
- 21 43. **Leungsakul, T., B.G. Keenan, B.F. Smets, and T.K. Wood.** 2005. TNT and
22 nitroaromatic compounds are chemoattractants for *Burkholderia cepacia* R34 and
23 *Burkholderia* sp. strain DNT. Appl. Microbiol. Biotechnol. **69**:321-325.
- 24 44. **Li, Z., and H. A. Scheraga.** 1987. Monte Carlo-minimization approach to the
25 multiple-minima problem in protein folding. Proc. Natl. Acad. Sci. USA
26 **84**:6611-6615.

- 1 45. **Liepinsh, E., M. Kitamura, T. Murakami, T. Nakaya, and G. Otting.** 1998.
2 Common ancestor of serine proteases and flavin-binding domains. *Nat. Struct. Biol.*
3 **5**:102-103.
- 4 46. **Lin, L. Y., T. Sulea, R. Szittner, V. Vassilyev, E. O. Purisima, and E. A.**
5 **Meighen.** 2001. Modeling of the bacterial luciferase-flavin mononucleotide complex
6 combining flexible docking with structure-activity data. *Protein Sci.* **10**:1563-1571.
- 7 47. **Link, A. J., D. Phillips, and G. M. Church.** 1997. Methods for generating precise
8 deletions and insertions in the genome of wild-type *Escherichia coli*: application to
9 open reading frame characterization. *J. Bacteriol.* **179**: 6228-6237.
- 10 48. **Lovering, A. L., E. I. Hyde, P. F. Searle, and S. A. White.** 2001. The structure of
11 *Escherichia coli* nitroreductase complexed with nicotinic acid: three crystal forms at
12 1.7 Å, 1.8 Å and 2.4 Å resolution. *J. Mol. Biol.* **309**:203-213.
- 13 49. **Muraki, T., M. Taki, Y. Hasegawa, H. Iwaki, and P. C. K. Lau.** 2003.
14 Prokaryotic homologs of the eukaryotic 3-hydroxyanthranilate 3,4-dioxygenase and
15 2-amino-3-carboxymuconate-6-semialdehyde decarboxylase in the 2-nitrobenzoate
16 degradation pathway of *Pseudomonas fluorescens* strain KU-7. *Appl. Environ.*
17 *Microbiol.* **69**:1564-1572.
- 18 50. **Murzin, A.G.** 1998. Probable circular permutation in the flavin-binding domain.
19 *Nat. Struct. Biol.* **5**: 101.
- 20 51. **Nishino, S. F., and J. C. Spain.** 2004. Catabolism of nitroaromatic compounds. p.
21 575-608. *In* J. L. Ramos. (ed.), *Pseudomonas* vol. 3. New York, USA; Kluwer
22 Acad/Plenum Publishers.
- 23 52. **Orii, C., S. Takenaka, S. Murakami, and K. Aoki.** 2004. A novel coupled
24 enzyme assay reveals an enzyme responsible for the deamination of a chemically
25 unstable intermediate in the metabolic pathway of 4-amino-3-hydroxybenzoic acid in
26 *Bordetella* sp. strain 10d. *Eur. J. Biochem.* **271**:3248-3254.

- 1 53. Pandey G., D. Paul., and R.K. Jain. 2003. Branching of *o*-nitrobenzoate
2 degradation pathway in *Arthrobacter protophormiae* RKJ100: identification of new
3 intermediates. FEMS Microbiol. Lett. **229**:231-236.
- 4 54. **Pandey, G. and R.K. Jain.** 2002. Bacterial chemotaxis toward environmental
5 pollutants: Role in bioremediation. Appl. Environ. Microbiol. **68**:5789-5795.
- 6 55. **Pang, Y. P., K. Xu, J. E. Yazal, and F. G. Prendergas.** 2000. Successful
7 molecular dynamics simulation of the zinc-bound farnesyltransferase using the
8 cationic dummy atom approach. Protein Sci. **9**:1857-1865.
- 9 56. **Parales, R.E.** 2004. Nitrobenzoates and aminobenzoates are chemoattractants for
10 *Pseudomonas* strains. Appl. Environ. Microbiol. **70**:285-292.
- 11 57. **Parales, R.E., M.D. Emig, N.A. Lynch, and D.T. Gibson.** 1998. Substrates
12 specificities of hybrid naphthalene and 2,4-dinitrotoluene dioxygenase enzyme
13 systems. J. Bacteriol. **180**:2337-2344.
- 14 58. **Parales, R.E., and C.S. Harwood.** 2002. Bacterial chemotaxis to pollutants and
15 plant derived aromatic molecules. Curr. Opin. Microbiol. **5**:266-273.
- 16 59. **Race, P.R., A. L. Lovering, R. M. Green, A. Osson, S. A. White, P. F. Searle, C.**
17 **J. Wrighton, and E. I. Hyde.** 2005. Structural and mechanistic studies of *Escherichia*
18 *coli* nitroreductase with the antibiotic nitrofurazone. Reversed binding orientations in
19 different redox states of the enzyme. J. Biol. Chem. **280**:13256-64.
- 20 60. **Russell, T. R., and S. C. Tu.** 2004. *Aminobacter aminovorans* NADH:flavin
21 oxidoreductase His140: a highly conserved residue critical for NADH binding and
22 utilization. Biochemistry **43**:12887-12893.
- 23 61. **Ryde, U.** 1999. Redesign of the coenzyme specificity in L-lactate dehydrogenase
24 from *Bacillus stearothermophilus* using site-directed mutagenesis and media
25 engineering. Protein Eng. **12**:851-856.
- 26 62. **Sambrook, J., E. F. Fritsh, and T. Maniatis.** 1989. Molecular cloning: a

1 laboratory manual, 2nd ed. Cold Spring Harbor Laboratory Press, Cold Spring Harbor,
2 N. Y.

3 63. **Schafer, A., A. Tauch, W. Jager, J. Kalinowski, G. Thierbach, and A. Puhler.**
4 1994. Small mobilizable multi-purpose cloning vectors derived from the *Escherichia*
5 *coli* plasmids pK18 and pK19: selection of defined deletions in the chromosome of
6 *Corynebacterium glutamicum*. *Gene* **145**:69-73.

7 64. **Schmidt, M. W., K. K. Baldrige, J. A. Boatz, S. T. Elbert, M. S. Gordon, J. H.**
8 **Jensen, S. Koseki, N. Matsunaga, K. A. Nguyen, S. Su, T. L. Windus, M. Dupuis,**
9 **and J. A. Montgomery.** 1993. General atomic and molecular electronic structure
10 system. *J. Comput. Chem.* **14**:1347-1363.

11 65. **Schreuder, H. A., P. A. Prick, R. K. Wierenga, G. Vriend, K. S. Wilson, W. G.**
12 **Hol, and J. Drenth.** 1989. Crystal structure of the p-hydroxybenzoate
13 hydroxylase-substrate complex refined at 1.9 Å resolution. Analysis of the
14 enzyme-substrate and enzyme-product complexes. *J. Mol. Biol.* **208**: 679-696.

15 66. **Simon, R., U. Priefer, and A. Pühler.** 1983. A broad host range mobilization
16 system for in vivo genetic engineering: transposon mutagenesis in Gram negative
17 bacteria. *Bio/Technology* **1**:784-791.

18 67. **Sivaraman, J., R. S. Myers, L. Boju, T. Sulea, M. Cygler, V. Jo Davison, and J.**
19 **D. Schrag.** 2005. Crystal structure of *Methanobacterium thermoautotrophicum*
20 phosphoribosyl-AMP cyclohydrolase HisI. *Biochemistry* **44**:10071-10080.

21 68. **Smith, S. P., K. R. Barber, S. D. Dunn, and G. S. Shaw.** 1996. Structural
22 influence of cation binding to recombinant human brain S100b: Evidence for
23 calcium-induced exposure of a hydrophobic surface. *Biochemistry* **35**:8805-8814.

24 69. **Somerville, C. C., S. F. Nishino, and J. C. Spain.** 1995. Purification and
25 characterization of nitrobenzene nitroreductase from *Pseudomonas pseudoalcaligenes*
26 JS45. *J. Bacteriol.* **177**:3837-3842.

- 1 70. **Tabor, S., and C. C. Richardson.** 1985. A bacteriophage T7 RNA
2 polymerase/promoter system for controlled exclusive expression of specific genes.
3 Proc. Natl. Acad. Sci. USA. **82**:1074-1078.
- 4 71. **Van den Heuvel, R.H.H., A. H. Westphal, A.J.R. Heck, M.A. Walsh, S. Rovida,**
5 **W.J. H. van Berkel, and A. Mattevi.** 2004. Structural studies on flavin reductase
6 PheA2 reveal binding of NAD in an unusual folded conformation and support novel
7 mechanism of action. J. Biol. Chem. **279**:12860-12867.
- 8 72. **Van der Meer, J.R., and V. Sentchilo.** 2003. Genomic islands and the evolution
9 of catabolic pathways in bacteria. Curr. Opin. Biotechnol. **14**:248-254.
- 10 73. **Wang, J., R. M. Wolf, J. W. Caldwell, P. A. Kollman, and D. A. Case.** 2004.
11 Development and testing of a general amber force field. J. Comput. Chem.
12 **25**:1157-1174.
- 13 74. **Yanisch-Perron, C., J. Vieira, and J. Messing.** 1985. Improved M13 phage
14 cloning vectors and host strains: nucleotide sequences of the M13mp18 and pUC19
15 vectors. Gene **33**:103-119.
- 16 75. **Yu, H. S., and M. Alam.** 1997. An agarose-in-plug bridge method to study
17 chemotaxis in the Archaeon *Halobacterium salinarum*. FEMS Microbiol Lett
18 **156**:265-269.
- 19 76. **Zylstra. G.J., S.-W. Bang, L.M. Newman, and L.L. Perry.** 2000. Microbial
20 degradation of mononitrophenols and mononitrobenzoates. p145-160. In J. C. Spain, J.
21 B. Hughes, and H.-J. Knackmuss (ed.), Biodegradation of nitroaromatic compounds
22 and explosives. Lewis Publishers, Boca Raton, Fla.

1 **Legends:**

2

3 Fig. 1. The two initial steps of 2-nitrobenzoate (2-NBA) metabolism by *P. fluorescens*
 4 strain KU-7 catalyzed by 2-NBA nitroreductase (NbaA) and 2-HABA mutase (NbaB)
 5 to produce 3-hydroxyanthranilate (3-HAA) via the formation of
 6 2-hydroxylaminobenzoate (2-HABA). The orientation and localization of *nbaA* and
 7 *nbaB* genes and flanking open reading frames (*orf*) are indicated by large open arrows
 8 beneath a restriction map. Sites of transposon Tn5-31Tp insertions producing the
 9 various KUM mutant strains are pinpointed. The numbering of *orfs* is according to
 10 Muraki et al (49). Orf11, 12, 13, 14, and 16 likely constitute an ABC transporter (22)
 11 for 2-NBA uptake. Orf15 is a putative FMN reductase. *nbaE* encodes a semialdehyde
 12 dehydrogenase as previously described (49). The cloned DNA fragments and probe
 13 regions are as indicated. The broken lines indicate the Tn5-31Tp DNA. *dhfrII* and *neo*
 14 are trimethoprim resistance- and kanamycin resistance-encoding genes, respectively.
 15 The DNA probes, labeled with DIG-11-dUTP are: a 1.8-kb HindIII-BamHI fragment
 16 (Probe 1) and a PCR-amplified DNA that is a *neo* gene sequence in Tn5-31Tp (Probe
 17 2). The PCR primers for Probe 2 are: 5'-GATCAAGAGACAGGATG-3' and
 18 5'-CACTCCTGCAGTTCG-3'.

19

20 Fig. 2. Coomassie blue-stained protein profiles of recombinant *E. coli* crude extracts
 21 separated on SDS-12% PAGE. Lane 1: molecular size markers as indicated alongside
 22 in kilodaltons. Lane 2, NbaA expressed in pSD*nbaA* lane 3, NbaB expressed in
 23 pSD*nbaB*; lane 4, *E. coli* cells containing the pSD80 vector only. Lane 5, NbaB
 24 expressed in pT7-5SD.NbaB. Lane 6, control *E. coli* JM109(DE3) containing the
 25 vector only. The positions of the expressed protein are indicated by circles.

26

1 Fig. 3. HPLC profiles of the reaction products generated by cell-free extracts
2 containing NbaA and/or NbaB. (A) Authentic standards 2-NBA, 2-HABA, 3-HAA,
3 and NADPH. (B) Identification of 2-HABA as a reaction product produced by
4 cell-free extracts containing NbaA. 0.25 μmol of 2-NBA and 0.96 μmol of NADPH
5 were incubated with NbaA in 30 mM potassium phosphate buffer (pH7.0) at the total
6 volume of 500 μl . Reaction mixture was analyzed by HPLC after 10 min incubation at
7 30°C. (C) Identification of 3-HAA as a reaction product produced by cell-free extracts
8 containing NbaA and NbaB. The reaction mixture, same as described in (B), was
9 incubated for 10 min at 30°C, and then aliquot of cell-free extracts containing NbaB
10 were added and further incubated for 10 min before the assay. In all cases, no product
11 formation was generated in the absence of the added heterologous enzymes.

12
13 Fig. 4. Modeled NbaA structure and interactions with FMN, NADPH and 2-NBA. (A)
14 Fold recognition based sequence alignment between NbaA and the currently
15 structurally characterized members (identified here by their PDB accession numbers at
16 <http://www.rcsb.org/>) of the NADH:FMN oxidoreductase-like structural family from
17 the FMN-binding split barrel fold. 1EJE – *Methanobacterium thermoautotrophicum*
18 FMN-binding protein MTH152; 1USF – *Thermus thermophilus* styrene
19 monooxygenase; 1IOS – *Archeoglobus fulgidus* ferric reductase; 1RZ1 – *Bacillus*
20 *thermoglucosidasius* flavin reductase PheA2; and 1WGB – *Thermus thermophilus*
21 probable flavoprotein. Secondary structure elements (α -helices, β -strands) of NbaA,
22 corresponding to its 3D homology model built based on this alignment, are indicated
23 above its sequence. The NbaA residues individually mutagenized to alanine in this
24 study are marked by closed circles color-coded according to the activity of the
25 corresponding mutants: red – inactive, magenta – residual activity, black – activity
26 comparable to wild-type. (B) Stereo view displaying the structural model of the NbaA

1 dimer. The trace of the NbaA main-chain, rendered schematically by its secondary
2 structure, is colored differently for the two monomers (green and cyan, respectively),
3 with the 10-residue insertion in the $\beta 5$ - $\alpha 2$ loop relative to the other members of the
4 fold family highlighted in red in one of the monomers. Ligands docked to NbaA are
5 shown only in one of the two equivalent binding sites of the homodimer, and colored
6 as: FMN – blue, NADPH – red, and Ni^{2+} – magenta. (C) Stereo view zooming in the
7 FMN binding site of NbaA. (D) Stereo view showing the modeled interactions of
8 NADPH with the FMN-bound NbaA. (E) Stereo view detailing the putative binding
9 mode of the 2-NBA substrate. In the latter three panels, the protein main-chain is
10 rendered as in panel (B), select protein residues and side chains are shown explicitly,
11 and the following color scheme is applied to the C atoms belonging to the various
12 displayed molecules: FMN – yellow, NADPH in panel (D) – light blue, 2-NBA in
13 panel (E) – magenta, protein – green or cyan. The other atom types are colored as: N –
14 blue, O – red, S – yellow, P – orange. Hydrogen bonds are shown with yellow dashed
15 lines, and metal ion hexa-coordination with black solid lines. The Ni^{2+} ion is
16 represented as a magenta sphere, and its two coordinating water molecules as red
17 spheres in panel (C).

18

19 Fig. 5. Proposed ping-pong mechanistic action of 2-nitrobenzoate nitroreductase in the
20 formation of 2-hydroxyaminobenzoic acid (2-HABA).

21

22 Fig. 6. NbaY is necessary for 2-NBA chemotaxis, as determined by A) swarm plate
23 assay, B) drop assay, and C) modified agarose-plug assay.

24

25 Fig. 7. Comparative organization and homology between the *nba* gene locus in *P.*
26 *fluorescens* strain KU-7 and the uncharacterized open reading frames encoded on a

1 large plasmid in *Polaromonas* sp. JS666. Major differences of the coding capacity are
2 notably at the extremities of the core biodegradative genes and in the spacing of the
3 intergenic regions.

4
5
6 Supplemental Fig. S1. The creation of in-frame deletion constructs of *nbaY*. The top
7 and second lines represent the two PCRs used to generate fragments (PCR1 and
8 PCR2) which will form an in-frame deletion of *nbaY* when fused. The PCR primers
9 *nbaY*-Ni and *nbaY*-Ci are complementary over 21 nucleotides (represented by the
10 broken lines) so that when two PCR products are mixed, the complementary regions
11 anneal and prime at the 3' overlapping region for a 3' extension of the complementary
12 strand. In the third line, the fused nucleotide molecule is amplified by PCR with
13 primers *nbaY*-No and *nbaY*-Co. Primers *nbaY*-No and *nbaY*-Co have *EcoRI* sites
14 incorporated into the 5' ends of both oligonucleotides (represented by the gray broken
15 lines) so that fusion product can be restriction digested and cloned into pK18*mobsacB*.

16
17 Supplemental Fig. S2. Multiple sequence alignment of NbaB. PoJS666 [*Polaromonas*
18 sp. JS666 acc. number: CP000317 (ABE46992)]; BxLB400 [*B. xenovorans* LB400 acc
19 number CP000270 (ABE31534)]; AzEbN1 [*Azoarcus* sp. EbN1 acc. number:
20 NC_006513 (YP_158576)]; RfDSM15236 [*Rhodospirillum rubrum* DSM 15236 acc.
21 number: CP000267 (ABD67975)]; PnbBTW3 [*P. putida* TW3 acc. number: AF292094
22 (AAG01543)]; PbnBYH102 [*Pseudomonas* sp. YH102 acc. number: AF187880
23 (AAF01448)]; and PbnBYH105 [*Ralstonia pickettii* acc. number: AF187879
24 (AAF01444)].

25
26 Supplemental Fig. S3. Multiple sequence alignment of NbaY. Pfpf-5 [*P. fluorescens*

TABLE 1. Bacterial strains and plasmids used in this study

Bacterial strain or plasmid	Relevant characteristics ^a	Source or reference
Strains		
<i>E. coli</i>		
BL21	F ⁻ <i>ompT hsdSB (r_B m_B) gal dcm</i>	Novagen
DH5α	<i>supE44 thi-1 recA1 hsdR17 endA1 gyrA (Nalr) Δ(lacIZYA-argF) U169 deoR [φ80dlac Δ(lacZ)M15]</i>	62
S17-1	<i>recA pro thi hsdR RP4-2-Tc::Mu-Km::Tn7 Tra⁻ Tp⁺ Sm^r</i>	66
XL1-blue	<i>recA1 endA1 gyrA96 thi hsdR17 supE44 relA1 [F' lacI^q ZM15 Tn10 (Tet^r)]</i>	10
<i>P. fluorescens</i>		
KU-7	Wild type, 2-NBA ⁺ , 4-HBA ⁺	27
KUM-9	<i>orf16::Tn5-31</i> Tp, 2-NBA ⁺ , 4-HBA ⁺	This study
KUM-19	<i>nbaA::Tn5-31</i> Tp, 2-NBA ⁺ , 4-HBA ⁺	This study
KUM-33	<i>nbaB::Tn5-31</i> Tp, 2-NBA ⁺ , 4-HBA ⁺	This study
KU7Δ7	<i>nbaY</i> deletion mutant	This study
Plasmids		
pKN31	Tn5-31 Tp transposon delivery plasmid; <i>mob</i> RP4 Km ^r Tp ^r	1
pK18 <i>mobsacB</i>	Negative selection vector, Km ^r	63
pREP1	Expression vector with T7 promoter, p15A origin, Cm ^r	57
pSD80	Expression vector with <i>tac</i> promoter, ColE1 origin, Ap ^r	68
pT7-5	Expression vector with T7 promoter, ColE1 origin, Ap ^r	69
pUC19	Cloning vector with <i>lac</i> promoter, ColE1 origin, Ap ^r	74
pNBA3	9.3-kb <i>Hin</i> dIII fragment from <i>P. fluorescens</i> strain KU-7 in pUC19; Ap ^r	49
pNBA5	6.2-kb <i>Eco</i> RI fragment from <i>P. fluorescens</i> strain KUM-19 in pUC19; Ap ^r , Tp ^r	This study
pNBA6	3.8-kb <i>Bam</i> HI fragment from <i>P. fluorescens</i> strain KUM-19 in pUC19; Ap ^r , Tp ^r	This study
pSD <i>nbaA</i>	<i>Eco</i> RI*- <i>Pst</i> I* fragment containing <i>nbaA</i> in pSD80	This study
pSD <i>nbaA</i> -N40A	Replacement of Asn40 by Ala in <i>NbaA</i> in pSD <i>nbaA</i>	This study
pSD <i>nbaA</i> -H63A	Replacement of His63 by Ala in <i>NbaA</i> in pSD <i>nbaA</i>	This study
pSD <i>nbaA</i> -H69A	Replacement of His69 by Ala in <i>NbaA</i> in pSD <i>nbaA</i>	This study
pSD <i>nbaA</i> -D76A	Replacement of Asp76 by Ala in <i>NbaA</i> in pSD <i>nbaA</i>	This study
pSD <i>nbaA</i> -H110A	Replacement of His110 by Ala in <i>NbaA</i> in pSD <i>nbaA</i>	This study
pSD <i>nbaA</i> -E113A	Replacement of Glu113 by Ala in <i>NbaA</i> in pSD <i>nbaA</i>	This study
pSD <i>nbaB</i>	<i>Eco</i> RI*- <i>Pst</i> I* fragment containing <i>nbaB</i> in pSD80	This study
pSD <i>nbaAnbaB</i>	pSD <i>nbaA</i> plus ribosome binding site at HindIII and NheI plus <i>nbaB</i> cloned at AscI and NheI	This study
pNbaΔY	<i>nbaY</i> deletion cassette in pK18 <i>mobsacB</i>	This study

^a*Eco* RI* and *Pst*I* are restriction endonucleases introduced by PCR design.

2-NBA+, growth on 2-NBA; 4-HBA+, growth on 4-hydroxybenzoate; 2-NBA-, no growth on 2-NBA

TABLE 2. NbaA activities in the cell-free extracts containing NbaA or its mutant proteins and the effect of FMN on their activities^a

NbaA	Specific activity			
	Without FMN		With FMN	
	U/mg ^b	%	U/mg	%
Wild-type	10.26 ± 0.23	100	31.73 ± 0.37	100
N40A	ND ^c	-	ND	-
H63A	7.44 ± 0.17	73	22.85 ± 0.33	72
H69A	0.20 ± 0.01	2	0.96 ± 0.03	3
D76A	ND	-	ND	-
H110A	3.38 ± 0.01	33	13.99 ± 0.38	44
E113A	ND	-	ND	-

^a FMN was added to the cell-free extracts containing NbaA and its mutants at the concentration of 5.0 mM, and it was preincubated for 5 min on ice prior to the assay.

^b One unit is the amount (in micromoles) of NADPH oxidized per minute. Results are the mean of three independent experiments with standard deviations noted.

^c Not detected

Fig. 1:

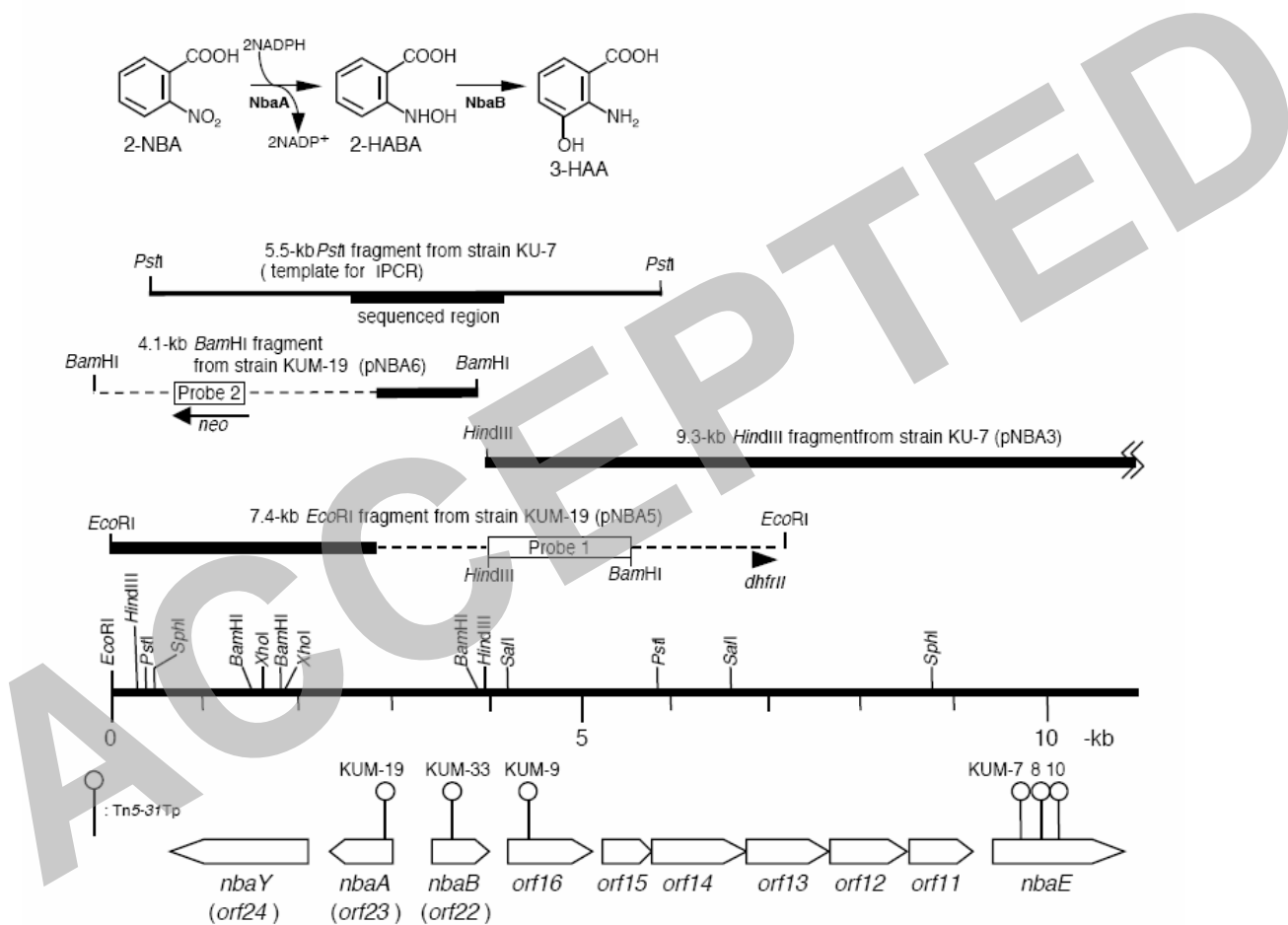


Fig. 2:

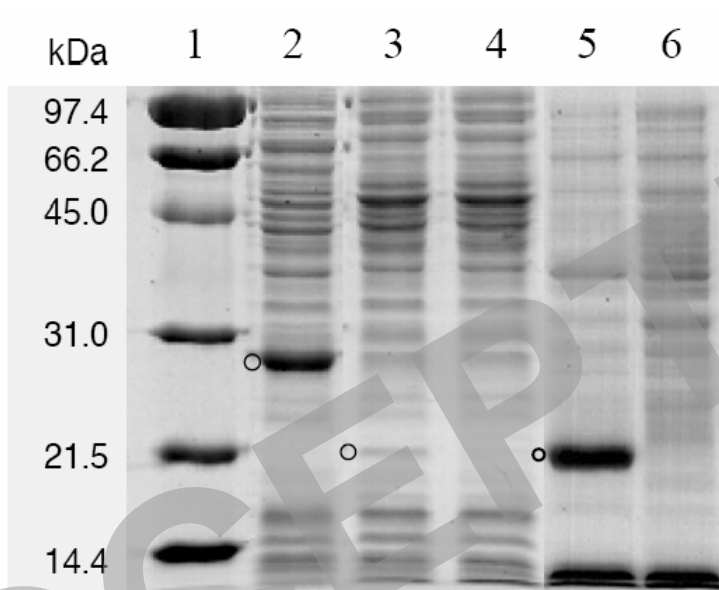


Fig. 3:

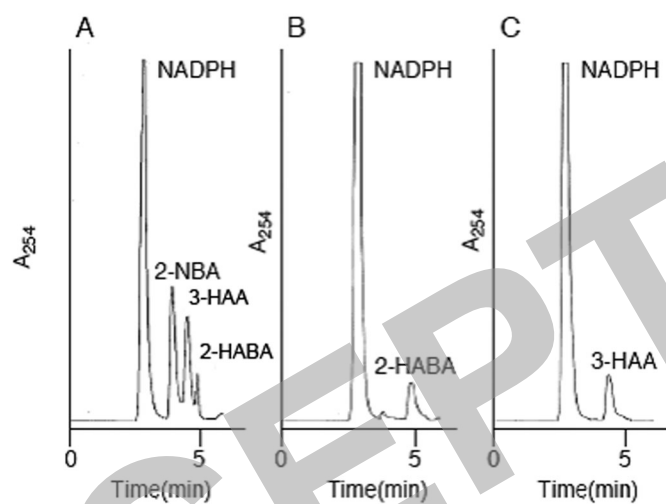


Fig. 5:

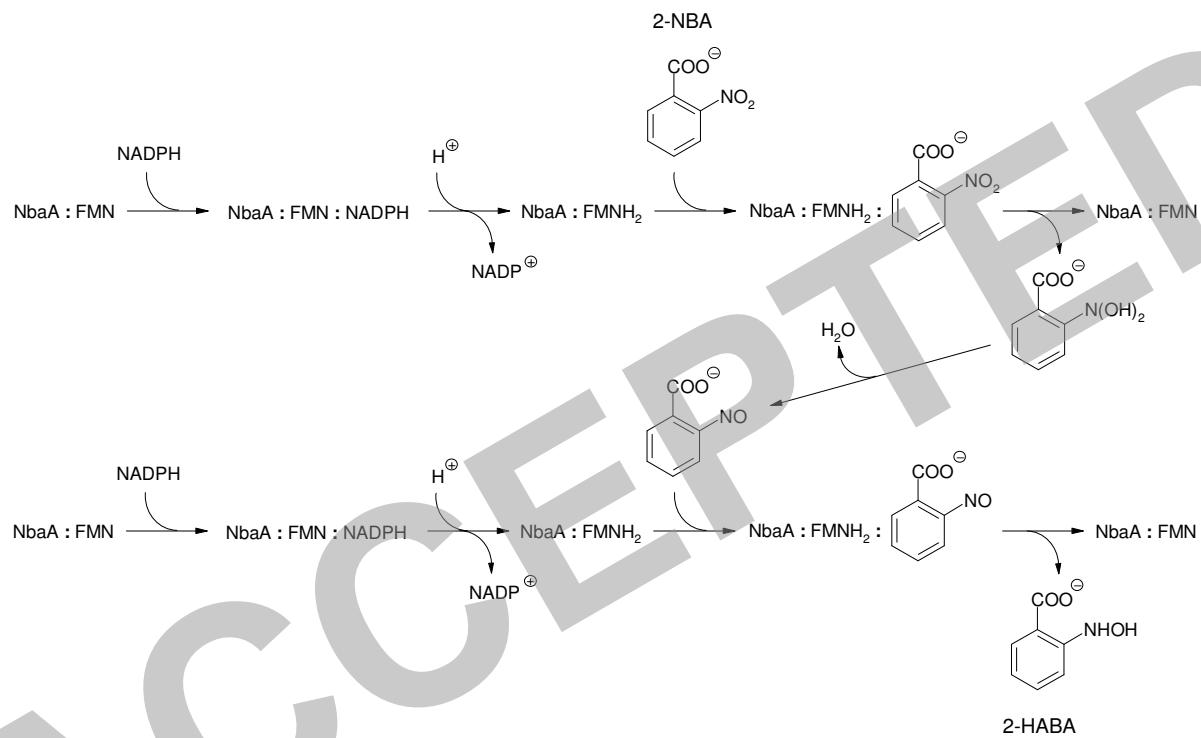


Fig. 6:

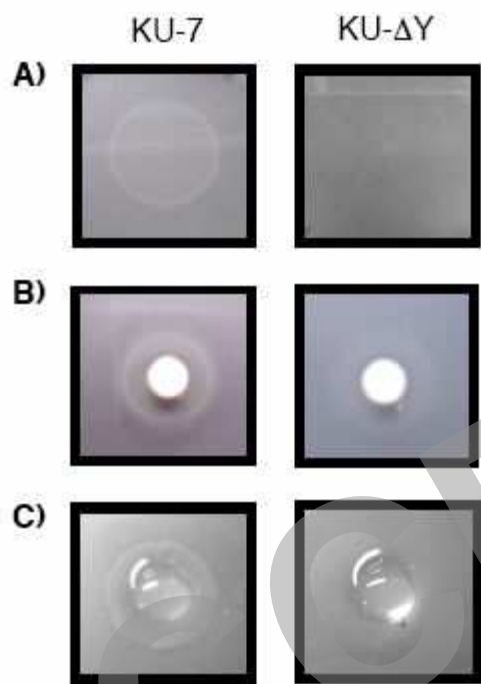


Fig 7:

